REPUBLIQUE ALGERINNE DEMOCRATIQUE ET POPULAIRE

Ministère de l'enseignement supérieur et de la recherche scientifique

Université El-Hadj Lakhder – Batna-

MEMOIRE

Présenté au Département de Physique

Faculté des Sciences

Pour l'obtention de diplôme de

Magister en Physique

Option : Physique Des Rayonnements

Par

Yassine RAHMANI

THEME

EFFETS DU MILIEU STELLAIRE SUR LES PHENOMENES NUCLEAIRES

Soutenu le / / 2008, devant le jury :

Président :	**Aissa BELGACEM-BOUZIDA**	**Professeur**	**U.Batna**
Rapporteur :	**Abdelhamid BOULDJEDRI**	**Professeur**	**U.Batna**
Examinateurs :	**Saad OUICHAOUI**	**Professeur**	**USTHB**
	Jamel MIMOUNI	**Professeur**	**U.Constantine**
	Said TOBBECHE	**M.C**	**U.Batna**

REPUBLIQUE ALGERINNE DEMOCRATIQUE ET POPULAIRE

Ministère de l'enseignement supérieur et de la recherche scientifique

Université El-Hadj Lakhder – Batna-

MEMOIRE

Présenté au Département de Physique

Faculté des Sciences

Pour l'obtention de diplôme de

Magister en Physique

Option : Physique Des Rayonnements

Par

Yassine RAHMANI

THEME

EFFECT OF STELLAR MEDIUM ON NUCLEAR PHENOMENA

Soutenu le / / 2008, devant le jury :

Président :	**Aissa BELGACEM-BOUZIDA**	**Professeur**	**U.Batna**
Rapporteur :	**Abdelhamid BOULDJEDRI**	**Professeur**	**U.Batna**
Examinateurs :	**Saad OUICHAOUI**	**Professeur**	**USTHB**
	Jamel MIMOUNI	**Professeur**	**U.Constantine**
	Said TOBBECHE	**M.C**	**U.Batna**

REMERCIEMENTS

Je dois plus à mon directeur de thèse, Monsieur le Professeur **Abdelhamid BOULDJEDRI** qu'à toute autre personne. Il m'a guidé, m'a inspiré, m'a encouragé. Et surtout, il a toujours cru en moi. Qu'il veuille bien trouver ici l'expression de mes vifs remerciements pour l'esprit de recherche et d'indépendance qu'il m a inculqué tout au long de cette aventure.

Monsieur le Professeur **Aissa BELGACEM- BOUZIDA**, de l'université de Batna, a bien voulu s'intéressé à cette étude et m'a fait l'honneur de présider le jury. Je le prie d'accepter ma profonde gratitude.

Je remercie Monsieur le Professeur **Saad OUICHAOUI**, de l'USTHB, pour l'intérêt qu'il a témoigné en vers ce travail en acceptant d'être membre de jury de ce mémoire.

A Monsieur le Professeur **Jamel MIMOUNI**, de l'université de Constantine, qui a accueilli mon travail avec bien vaillance et intérêt, je tien à exprimer ma profonde reconnaissance.

Que Monsieur **Said TOBBECHE**, maître de conférences à l'université de Batna, trouve ici l'expression de ma très sincère reconnaissance, de bien vouloir faire partie de la commission d'examen.

Enfin, je remercie aussi ceux qui ont contribué de prés ou de loin à la réalisation et l'aboutissement de ce travail.

RESUME DETAILLE DU TRAVAIL REALISE

L'étude de la production d'énergie dans les étoiles et leur évolution nécessite une maîtrise des phénomènes nucléaires. Ces derniers ont été principalement étudiés dans les conditions physiques terrestres. L'astrophysique nucléaire étend ces études aux conditions physiques qui règnent dans les étoiles.

Dans ce mémoire de Magister nous nous avons proposé d'étudier l'effet du milieu stellaire sur les réactions nucléaires et les propriétés de la matière nucléaire stellaires.

Le troisième chapitre de ce mémoire est consacré à l'effet d'écrantage atomique et son impact sur les réactions nucléaire de fusion d'intérêt astrophysique, dont on a proposé un modèle pour calculer la densité électronique en présence de cet effet (BES MODEL- Batna Electron Screening Model). L'expression du potentiel obtenu à partir de la forme de la densité proposé ; montre des termes de correction en faisant une comparaison avec celui obtenu par T. Liolios, ce qui est montré en équation (3.21) et (3.22) successivement

$$V^{BES}(r) = \frac{Z_1 Z_2 e^2}{r} - \frac{6}{50}\frac{Z_1 Z_2 e^2}{a_0}\left[1 - \frac{4}{5}\left(\frac{r}{a_0}\right)^2 + \frac{21}{100}\left(\frac{r}{a_0}\right)^4 - \frac{1}{20}\left(\frac{r}{a_0}\right)^6 + \frac{1}{144}\left(\frac{r}{a_0}\right)^8\right]$$

$$V^{Lio}(r) = \frac{Z_1 Z_2 e^2}{r} - \frac{2\,Z_1 Z_2 e^2}{a_0}\left[\frac{3}{2} - \frac{5}{2}\left(\frac{r}{a_0}\right)^2 + \frac{39}{20}\left(\frac{r}{a_0}\right)^4\right]$$

Dans la deuxième partie dans ce chapitre, le facteur astrophysique pour les états excités est donné par l'équation (3.70) comme suit

$$S(E) = (5.5 - 3.1E + 1.4E^2)\exp\left(\pi\eta\frac{U_e}{E}\right)$$

la représentation graphique de $S(E)$ est faite pour l'approximation linéaire ainsi que pour l'approximation quadratique, où U_e est l'énergie due au présence des électrons. La valeur numérique de U_e calculé est proche de celle calculé par T. Liolios. Finalement une comparaison a été faite entre les deux modèles de calcules.

Dans le quatrième chapitre nous avons étudié l'effet d'un champ magnétique très intense sur les réactions de fusion thermonucléaire (D-D). Commençant par donner une fonction d'essai -donnée par l'équation (4.28)- afin d'avoir la forme analytique de l'énergie de l'état fondamentale, les valeurs numériques de cette dernière sont obtenues après avoir minimiser

l’intégral (4.31) pour chaque valeur du champ magnétique, après ; nous avons calculé le potentiel électrique modifié par le champ magnétique en résolvant l’équation de Poisson (4.46), afin de prédire l’effet de ce dernier sur la section efficace en calculant le facteur d’amélioration f. le facteur f est représenté pour chaque valeur du champ magnétique, une comparaison avec [Hey 96] montre un saut dans la valeur de f pour $B = 10^{12}G$, ce qui est justifié par le choix de la fonction d’essai.

Le cinquième chapitre, est une étude sur l’effet du champ magnétique dans l’atmosphère des magnétars, dont nous nous sommes limité à l’étude de la désintégration alpha, et avons donné la forme analytique du potentiel en présence d’un champ magnétique –équation (5.28), ce qui nous a permit de dériver la forme analytique de f - équation (5.29)-, l’effet du champ magnétique sur la barrière Coulombienne est illustré dans les figures.5.3,5.4,5.5,5.6, et les valeurs numérique de f sont données dans le tableau (5.2), ce dernier montre l’influence sur la période de la désintégration qui croit avec le champ magnétique, nous avons aussi étudié l’effet du plasma sur la désintégration alpha en tenant compte du terme non linéaire dans l’équation de Poisson (5.36), le potentiel obtenu est donné par l’équation (5.44), ce dernier indique l’abaissement de la barrière Coulombienne en présence d’un plasma dense.

TABLE OF CONTENTS

CHAPTER 3

ATOMIC SCREENING IN ASTROPHYSICAL NUCLEAR REACTIONS

CHAPTER 4

MAGNETICALLY CATALYZED SCREENING IN FUSION REACTIONS

Introduction

It is in the nature of astrophysics that many of the processes and most of the objects one tries to understand are physically inaccessible. Thus, it is important that those aspects that can be studied in the laboratory be rather well understood.

The main goals of nuclear astrophysics have been to probe the interiors of stars, stellar explosions, the early moments of cosmic expansion, and the formation and evolution of galaxies and cosmic structure by measurement and application of the relevant nuclear physics. The approach to these goals have generally been from three directions: 1) Careful measurements of the relevant nuclear reactions; 2) Detailed computer models of the relevant astrophysical environments; and 3) Observations of the relevant terrestrial and extra-terrestrial atomic and isotopic abundances. These approaches provide not only insight into the formation and evolution of the elements, but are also pillars upon which a variety of cosmological models as well as models for physics beyond the standard model of particle physics can stand or fall.

However, studying the nuclear phenomena in the terrestrial environment is different from the stellar environment, because there are several factors, such as the density of the matter, the intensity of the magnetic field, etc….. , so more effects will occur. The electron screening effect on fusion reaction addresses one such aspect.

In the first chapter, an overview of nuclear astrophysics is given, showing its goal and its relevance in the understanding of the universe.

In the second chapter, the astrophysical nuclear reactions, and some generalities about nuclear rates and cross section will be given.

In the third chapter, the effect of atomic screening and its effect on astrophysical nuclear reactions be studying. We have first proposed an improvement of the simple quadratic model. Then calculation based on the electron wave function has been extended to excited states, subsequently the atomic screening effect on astrophysical factor for the reaction $^{3}\mathrm{He}(^{3}\mathrm{He}, 2\mathrm{p})^{4}\mathrm{He}$ has been evaluated.

In the fourth chapter, the enhanced atomic screening by a strong magnetic field is reviewed. A new solution has been obtained and subsequently its effect on nuclear reaction has been calculated.

In the fifth chapter, we have applied the result of chapter three to evaluate the reductions of the alpha radioactivity. The effect of non linear plasma shielding on such half lives has also been studied.

CHAPTER 1

ELEMENTS OF NUCLEAR ASTROPHYSICS

1.1 INTRODUCTION

Nuclear Astrophysics is the study of the nuclear processes which drive the birth, evolution and death of stars. The current cosmological belief is that the nuclei which make up the majority of matter were first made from nucleons created a short time after the beginning of the Universe, in the expanding fireball we call the Big-bang, and later forged in the interiors of stars and stellar explosions [Arn00].

It is of significant and enduring interest to Mankind to piece together the picture of our evolution from the very first times. In particular, we now know that almost all of the material from which our planet was created was made in a vast series of nuclear reactions inside stars, and spread throughout the interstellar medium via stellar outbursts and energetic explosions. Astrophysicists have modeled these processes in the hope of explaining the isotopic abundances we see today on our Earth, around the Solar system, in meteoric remount and in astronomical observations of other stellar systems and the interstellar medium, in the hope of tying together a comprehensive understanding of the series of events leading to our present condition. Also of interest are the physical constraints placed on the energy generation and lifetimes of stars resulting from the detailed study of the realm of nuclear interactions, leading to predictive models and observational tools useful in cosmology, the study of the large-scale evolution of the Universe [Arn00].

Currently, much research is being done into the reaction rates of various nuclear processes in low energy stellar environments, such as Hydrogen burning in Main sequence stars and red giants. Nuclear cross-sections are measured at the lowest possible experimental energy, and then extrapolations are made to stellar energies, which tend to be still lower. Also subjects of active research are the higher energy processes of hydrogen burning in the hot CNO cycles and their breakout.

The breakout reactions from the hot CNO cycle are currently being paid much experimental attention. Of particular importance in Nuclear Astrophysics however, is the study of the specifics of the rapid proton process. Questions which need to be answered are: What are the key contributing reactions in the rp-process at various temperatures? What are typical r p-process sites:

does it occur in X-ray busters only, and if so does the envelope escape into the interstellar medium providing a nucleosynthesis source? Do rp-process reactions occur in novae, where we know the envelope escapes? How much of the nucleosynthesis of proton-rich nuclei can be accounted for by these rp-process scenarios?

1.1. The Hertzsprung – Russell Diagram (HRD):

The Hertzsprung-Russell diagram (usually referred to by the abbreviation H-R diagram or HRD, also known as a colour-magnitude diagram, or CMD) gives the relationship between absolute magnitude, luminosity, classification, and effective temperature of stars. The diagram was created virca 1910 by Ejnar Hertzsprung and Henry Norris Russell, and represented a huge leap forward in understanding stellar evolution, or the 'lives of stars'.

There are several forms of the Hertzsprung-Russell diagram, and the nomenclature is not very well defined. The original diagram displayed the spectral type of stars on the horizontal axis and the absolute magnitude on the vertical axis. The first quantity (i.e. spectral type) is difficult to determine unambiguously and is therefore often replaced by the B-V colour index of the stars. This type of diagram is called a Hertzsprung-Russell diagram, or colour-magnitude diagram, and it is often used by observers. However, colour-magnitude diagram is also used in some cases to describe a plot with the vertical axis depicting the apparent, rather than the absolute, magnitude. Another form of the diagram plots the effective temperature of the star on one axis and the luminosity of the star on the other. This is what theoreticians calculate using computer models that describe the evolution of stars. This type of diagram should probably be called temperature-luminosity diagram, but this term is hardly ever used, the term Hertzsprung-Russell diagram being preferred instead. Despite some confusion regarding the nomenclature, astrophysicists make a strict distinction between these types of diagrams.

The H-R diagram can be used to define different types of stars and to match theoretical predictions of stellar evolution using computer models with observations of actual stars. It is then necessary to convert either the calculated quantities to observables, or the other way around, thus introducing an extra uncertainty.

Most of the stars occupy the region in the diagram along the line called main sequence. During that stage stars are fusing hydrogen in their cores. The next concentration of stars is on the horizontal branch (helium fusion in the core and hydrogen burning in a shell surrounding the core).

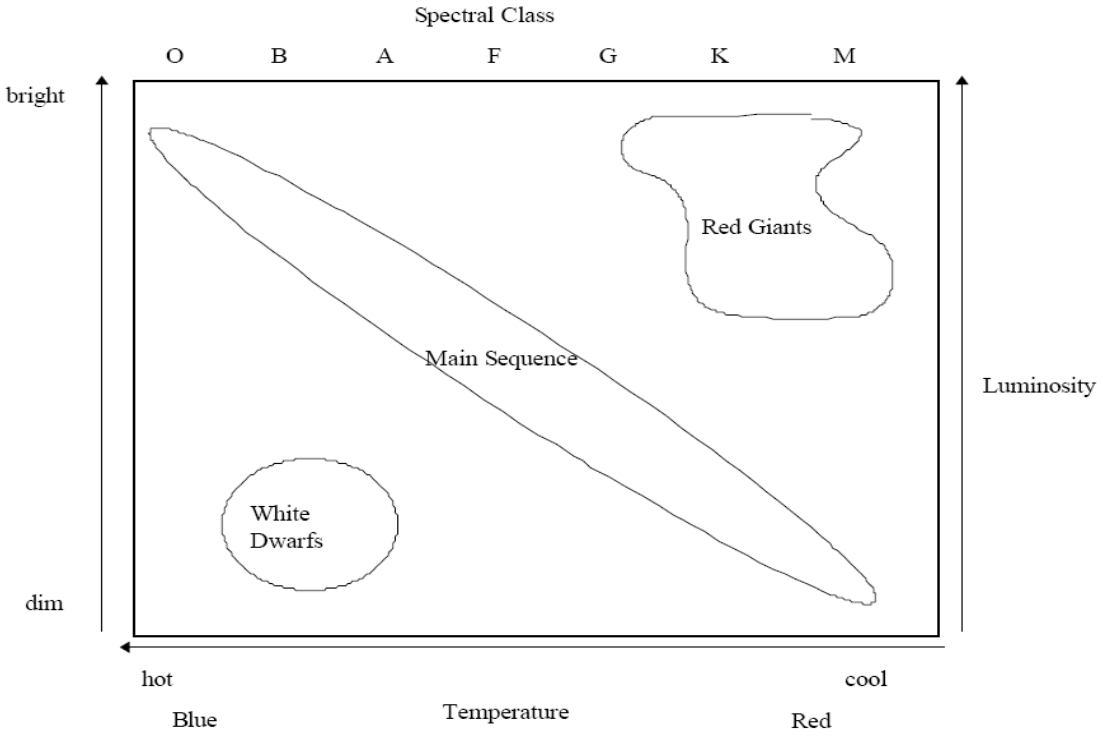

Fig 1.1. *H-R Diagram.*

The largest group of stars in Figure 1 is that labeled Main Sequence. The main sequence is common to all H-R diagrams and is the longest stage of evolution for any star. A star on the main sequence derives its energy almost entirely from nuclear reactions involving the conversion of hydrogen to helium via fusion. A star spends most of its life on the main sequence. From the diagram we see that the brighter a main sequence star is, the hotter it is. The hotter main sequence stars are also bluer and more massive. The cooler, dimmer main sequence stars are redder and less massive. Although it is not obvious, the hotter, brighter, more massive, and bluer a star is, the less time it spends on the main sequence. It is important to note that *stars do not move up and down the main sequence*. The position of a star on the main sequence is uniquely determined by its mass.

The next region of interest in Figure 1 is the group of stars labeled Red Giants.1 The red giant phase of stellar evolution follows the main sequence phase. When the hydrogen is nearly exhausted in the central core of a star, the star begins to undergo a cataclysmic set of convulsions. During this process, core temperature, pressure and density increase within the star. Energy released during this process causes the outer parts of the star to swell to enormous proportions. The star, as a whole, becomes less dense since all but the central core is expanding. This expansion of the outer regions of the star results in surface cooling and results in their red appearance. The energy being released by the core heats up the hydrogen in the areas surrounding it to extremely

high temperatures. This accelerates hydrogen fusion and the production of helium, causing the star to increase in luminosity. After leaving the main sequence these stars move to the upper right side of the H-R diagram (low temperature, high luminosity). Red giants are, therefore, characterized by very large diameters and relatively low surface temperatures. Their large diameters, and consequently their large surface areas, make them relatively bright.

The final group of stars in Figure 1 are White Dwarfs. These stars are at the end of the line in terms of stellar evolution. Near the end of a star's life, as it begins to exhaust its supply of energy, it begins to shrink. During this process the star may ultimately attain an enormous density. White dwarfs are compact objects about the size of Moon but containing about mass of the sun. Although white dwarf stars are extremely hot, they are not very bright because of their compact size. White dwarf stars have very high densities (roughly that of the nucleus of an atom). This is possible because the constituent atoms of the gases residing in the interior of these stars are completely *ionized*, i.e., stripped of all electrons. Most of the mass of an atom (~99.975%) is concentrated in the nucleus, but most of the volume is occupied by orbiting electrons. With the electrons stripped away, it is possible to pack nuclei very close together resulting in a substance of extremely high density. The density of a typical white dwarf star is, for example, over a million times that of water.

There are two other possible end states in stellar evolution: neutron stars and black holes. Neither of these are luminous enough to appear in the H-R diagram.

To summarize, there are three main classes of stars on the H-R diagram. A star begins its evolution at a point on the main sequence determined by its mass, matures into a red giant stage, and can end its life as a white dwarf.

.

1.2.Nucleosynthesis:

The abundance of a chemical element measures how relatively common the element is, or how much of the element there is by comparison to all other elements. Abundance may be variously measured by the mass-fraction (the same as weight fraction), or mole-fraction (fraction of atoms, or sometimes fraction of molecules, in gases), or by volume fraction. Measurement by volume-fraction is a common abundance measure in mixed gases such as atmospheres, which is close to molecular mole-fraction for ideal gas mixtures (i.e., gas mixtures at relatively low densities and pressures).

There are various methods for determining the abundances of elements in the unverse, wether directly (meteorites, terrestrial material, ….), or by interpretation of the stellar spectra. The

last method is fundamental in astrophysics, it is based on the theory of quantified model of the atom.

The Earth is formed from the same cloud of matter that formed the Sun, but the planets acquired different compositions during the formation and evolution of the solar system. The schematic curve of atomic abundances is given in (Fig.1.2)

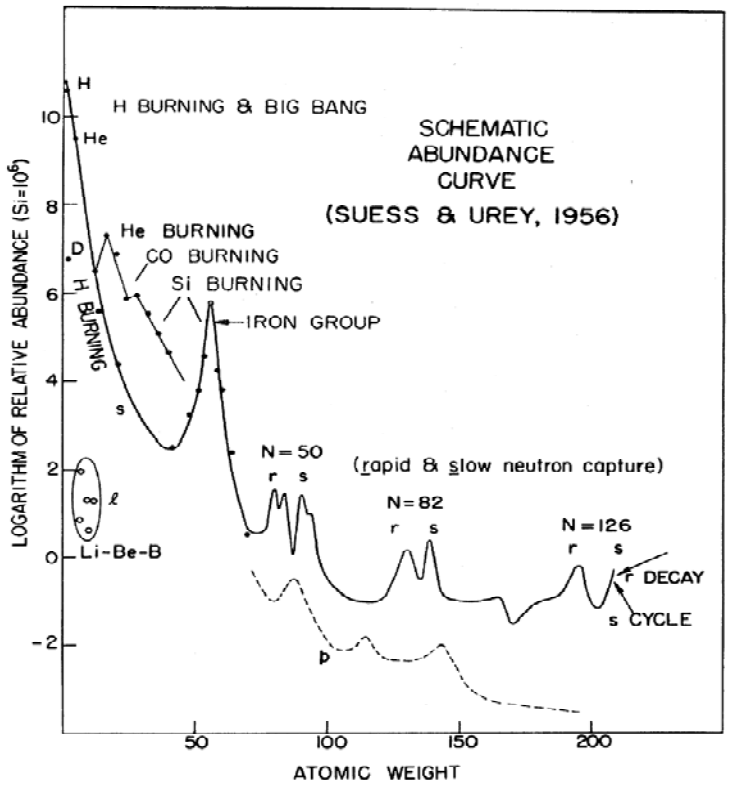

Figure 1.2. *The abundances of the elements in the solar system.*

We can given some comments about the curve in Fig.1.3:

a) Hydrogen and helium are estimated to make up roughly 98 % of all the matter in the universe.
b) The nuclear abundances generally decrease with increasing atomic wieght.
c) A large peak is encountered for $A = 56$ (iron).

1.2.1. Hydrogen burning

The beginning of star formation is with the gravitational collapse of a cloud composed of hydrogen, helium and traces of other chemical elements. Then the cloud contracts slowly in a state close to hydrostatic equilibrium; half the gravitational energy released is lost as radiation and the other heats up the cloud. The contraction will continue until the activation of a source of energy

other than gravity. The first is the thermonuclear fusion of proton with light nuclei such as D, Li, Be and B.

The net effect of hydrogen burning is to transform protons into ${}_2^4He$ nuclei, this transformation can only be effected by a nuclear weak process, which the most is $p \rightarrow n + e^+ + v_e$, in this case the result is

$$4p \rightarrow {}^4He + 2e^+ + 2v_e \tag{1.1}$$

Hydrogen burning would be a straightforward and rapid process, if a bound state of two protons existed. Such a state would be an isotope of helium, ${}^2He$, and hydrogen would begin to burn via the electromagnetic reaction

$$p + p \rightarrow {}^2He + \gamma \tag{1.2}$$

1.2.1.1 The proton-proton chain

The underlying mechanism for this reaction is that one of the interacting protons undergoes inverse beta decay, and the neutron produced is then bound to the other proton to form a deuteron. There are three sequences of reactions which form the main branches of the proton-proton chain. These branches are shown in Fig 1.3.

The pp-I chain is:

$$p + p \rightarrow d + e^+ + v_e \tag{1.3}$$

$$d + p \rightarrow {}^3He + \gamma \tag{1.4}$$

$${}^3He + {}^3He \rightarrow {}^4He + p + p \tag{1.5}$$

In the pp-II chain ${}^3He$ produced by (1.3) and (1.4) undergoes different reaction chain leading to ${}^4He$:

$${}^3He + {}^4He \rightarrow {}^7Be + \gamma \tag{1.6}$$

$${}^7Be + e^- \rightarrow {}^7Li + v_e \tag{1.7}$$

$${}^7Li + p \rightarrow {}^4He + {}^4He \tag{1.8}$$

Finally in less then 0.02% ^{7}Be produced by (1.6) can start the PP III chain by absorbing a proton (instead of e^{-} capture) to generate ^{4}He in three steps.

The pp-III chain is:

$$p + {}^{7}Be \rightarrow {}^{8}B + \gamma \tag{1.9}$$

$$^{8}B \rightarrow {}^{8}Be + e^{+} + \nu_{e} \tag{1.10}$$

$$^{8}Be \rightarrow {}^{4}He + {}^{4}He \tag{1.11}$$

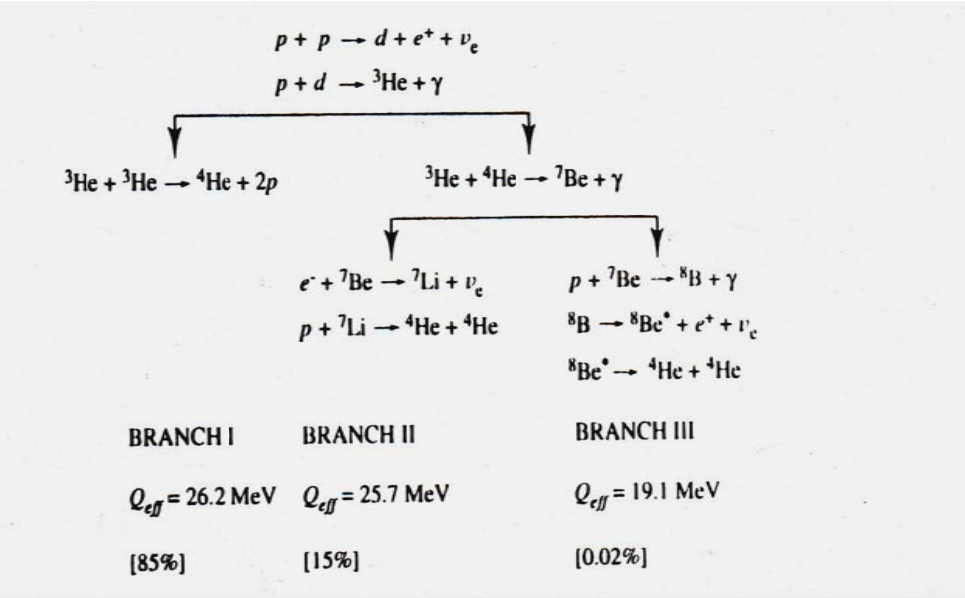

Fig 1.3. *The three branches of the pp chain.*

1.2.1.2. The CNO cycle:

The pp chain can account for hydrogen burning in main sequence stars with masses comparable to the sun, the CNO cycle- illustrated in Fig 1.4.- depends on the presence of small quantities of carbon, while is produced in earlier generations of stars by helium burning. This cycle becomes active in stars at temperatures in excess of around $10^{7}K$. The CNO cycle begins with the radiative proton capture on ^{12}C. The cycle then proceeds via a series of proton-capture and β-decays.

$$^{12}C(p,\gamma)^{13}N(\beta^{+},\nu_{e})^{13}C(p,\gamma)^{14}N(p,\gamma)^{15}O(\beta^{+},\nu_{e})^{15}N(p,\alpha)^{12}C \tag{1.12}$$

The recult of this process is the conversion of four protons into a helium nucleus, with the release of energy. The carbon, nitrogen and oxygen nuclei are used as catalysts, their relative abundances remaining unchanged during the process.

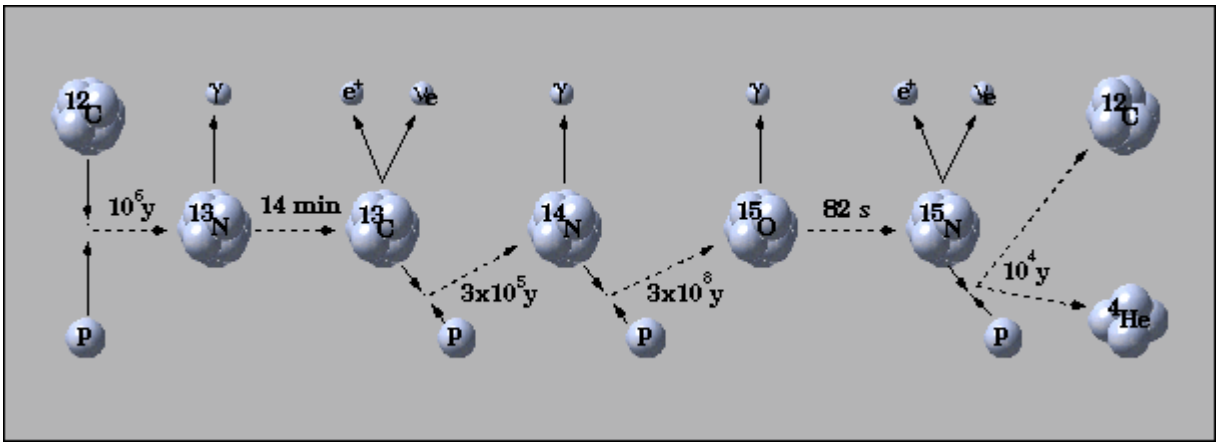

Fig 1.4. *The CNO Cycle.*

1.2.2. Helium burning:

Helium burning produces two vitally important chemical elements, namely oxygen and carbon. Moreover, 0.85% and 0.39% of matter in the solar system is composed of oxygen and carbon, only hydrogen and helium are more abundant. Thus, helium burning is an important process [Aud72].

The helium burning reactions are:

$$3\ {}^{4}He \rightarrow {}^{12}C \tag{1.13}$$

$${}^{12}C + {}^{4}He \rightarrow {}^{16}O + \gamma \tag{1.14}$$

$${}^{14}N + {}^{4}He \rightarrow {}^{18}F + \gamma \rightarrow {}^{18}O + e^{-} + v \tag{1.15}$$

$${}^{18}F \rightarrow {}^{18}O + e^{-} + v \tag{1.16}$$

The last chain, can be considered as a very good source of the neutron by the next reactions:

$${}^{18}O + {}^{4}He \rightarrow {}^{21}Ne + n \tag{1.17}$$

$$^{21}Ne + \alpha \rightarrow {}^{24}Mg \quad (1.18)$$

$$^{18}O + {}^{4}He \rightarrow {}^{22}Ne + \gamma \quad (1.19)$$

$$^{22}Ne + {}^{4}He \rightarrow {}^{25}Mg + n \quad (1.20)$$

$$^{22}Ne + {}^{4}He \rightarrow {}^{26}Mg + \gamma \quad (1.21)$$

$$^{25}Mg + {}^{4}He \rightarrow {}^{28}Si + n \quad (1.22)$$

$$^{26}Mg + {}^{4}He \rightarrow {}^{29}Si + n \quad (1.23)$$

1.2.3 The Carbon burning:

The Carbon burning process is a set of nuclear fusion reactions that take place in massive stars that have used up the lighter elements in their cores. It requires high temperatures ($6 \times 10^8 K$) and densities about ($2 \times 10^8 kg/m^3$) the principal reactions are:

$$^{12}C + {}^{12}C \rightarrow {}^{24}Mg + \gamma \quad (1.24)$$

$$^{12}C + {}^{12}C \rightarrow {}^{23}Na + p \quad (1.25)$$

$$^{12}C + {}^{12}C \rightarrow {}^{20}Ne + {}^{4}He \quad (1.26)$$

$$^{12}C + {}^{12}C \rightarrow {}^{23}Mg + n \quad (1.27)$$

Carbon burning starts when helium burning ends. During helium fusion, stars build up an inert core rich in carbon and oxygen. Once the helium density drops below a level at which He bruning can be sustained, the core collapses due to gravitation. This decrease in volume raises temperature and density of the core up to the carbon ignition temperature. This will raise the star's temperature around the core allowing it to burn helium in a shell around the core. The star increases in size and becomes a red supergiant.

1.2.4. Oxygen burning

These reactions start when C-burning ends, it requires a high temperature ($4.5 \times 10^{9°}K$). The principal reactions are

$$^{16}O + {}^{16}O \rightarrow {}^{32}S + \gamma \quad (1.28)$$

$$^{16}O + {}^{16}O \rightarrow {}^{31}P + p \quad (1.29)$$

$$^{16}O + {}^{16}O \rightarrow {}^{28}Si + {}^{4}He \quad (1.30)$$

$$^{16}O + {}^{16}O \rightarrow {}^{24}Mg + 2\,{}^{4}He \quad (1.31)$$

$$^{16}O + {}^{16}O \rightarrow {}^{31}S + n \quad (1.32)$$

1.2.5. Photodesintegration

It is a physical process in which extremely high enegy gamma rays interact with an atomic nucleus and cause it to enter an excited state. This process is essentially the reserve of nuclear fusion, where lighter elements at high temperatures combine together forming heavier elements and releasing energy. Photodisintegration is responsible for the nucleosynthesis, the most important interactions are:

$$\gamma + {}^{28}Si \rightarrow {}^{24}Mg + {}^{4}He \quad (1.33)$$

$$^{28}Si + {}^{4}He \rightarrow {}^{32}S + \gamma \quad (1.34)$$

$$^{24}Mg + \gamma \rightarrow {}^{20}Ne + {}^{4}He \quad (1.35)$$

$$^{20}Ne + \gamma \rightarrow {}^{16}O + {}^{4}He \quad (1.36)$$

After high-mass stars have nothing but sulfur and silicon in their cores, they further contract until their cores reach in the range of 2.7–3.5 GK; silicon burning starts at this point. Silicon burning entails the alpha process which creates new elements by adding the equivalent of one helium nucleus (two protons plus two neutrons) per step in the following sequence

$$^{28}Si + {}^{4}He \rightarrow {}^{32}S \quad (1.37)$$

$$^{32}S + {}^{4}He \rightarrow {}^{36}Ar \quad (1.38)$$

$$^{36}Ar + {}^{4}He \rightarrow {}^{40}Ca \quad (1.39)$$

$$^{40}Ca + {}^{4}He \rightarrow {}^{44}Ti \quad (1.40)$$

$$^{44}Ti + {}^{4}He \rightarrow {}^{48}Cr \quad (1.41)$$

$$^{48}Cr + {}^{4}He \rightarrow {}^{52}Fe \quad (1.42)$$

$$^{52}Fe + {}^{4}He \rightarrow {}^{56}Ni \quad (1.43)$$

The entire silicon-burning sequence lasts about one day and stops when nickel–56 has been produced. Nickel–56 (which has 28 protons) has a half-life of 6.02 days and decays via beta radiation (beta plus decay, which is the emission of a positron) to cobalt–56 (27 protons), which in turn has a half-life of 77.3 days as it decays to iron–56 (26 protons). However, only minutes are available for the nickel–56 to decay within the core of a massive star. At the end of the day-long silicon-burning sequence, the star can no longer convert mass into energy via nuclear fusion because a nucleus with 56 nucleons has the lowest mass per nucleon (proton and neutron) of all the elements in the alpha process sequence.

Fig.1.5 shows the binding energy of various elements. Increasing values of binding energy can be thought of in two ways: 1) it is the energy required to remove a nucleon from a nucleus, and 2) it is the energy released when a nucleon is added to a nucleus. As can be seen, light elements such as hydrogen release large amounts of energy (a big increase in binding energy) as nucleons are added—the process of fusion. Conversely, heavy elements such as uranium release energy when nucleons are removed—the process of nuclear fission. Although nuclei with 58 and 62 nucleons have the very lowest binding energy, fusing four nucleons to nickel–56 to produce the next element — zinc–60 — actually requires energy rather than releases any. Accordingly, nickel–56 is the last fusion product produced in the core of a high-mass star.

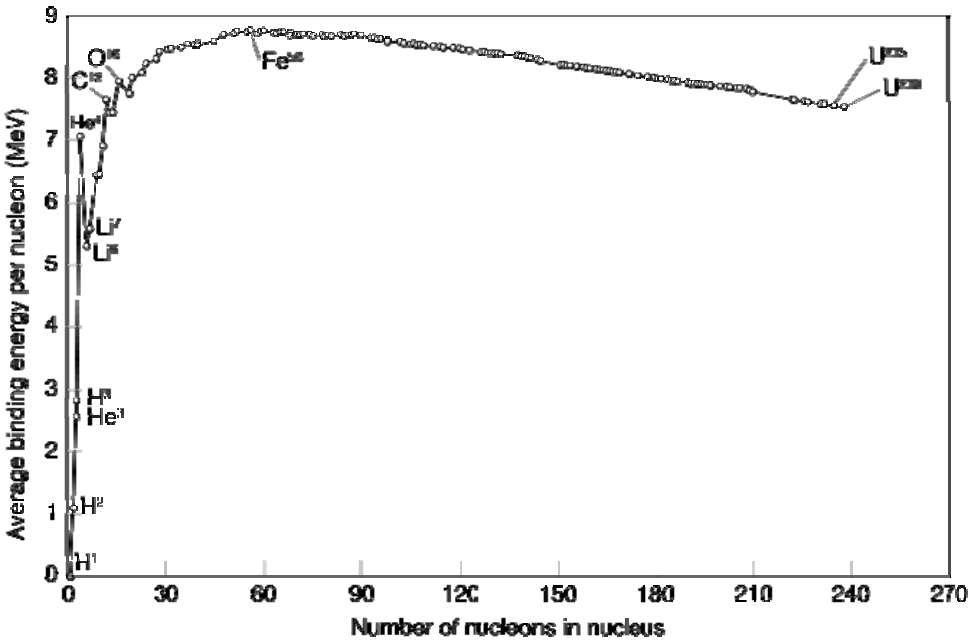

Fig 1.5. *the binding energy of various elements.*

1.2.6. r, s and p process:

Two neutron-capture processes, the slow (s) process and the rapid (r) process, are thought to be responsible for the synthesis of the heavy elements beyond iron. The s-process is a non-explosive process, while the r-process is thought to occur only in explosive scenarios. The r-process is thought to be responsible for the nucleosynthesis of the actinides, since these cannot be created via the s-process.

During the explosion, there is a large neutrino flux from the core, and also a large flux of neutrons. In this neutron-rich environment, the r- and s-processes can occur, synthesising massive neutron-rich matter via staggered radiative-capture-beta-decay path (See Fig 1.6). The s-process can synthesise isotopes up to ^{209}Bi. It is thought that the r-process can account for a large fraction of the nucleosynthesis of neutron-rich isotopes up to the Uranium island. The r-process only occurs after collapse of the stars because the density and neutron ux need to be extremely high. During the r-process and s-process, all the nucleosynthesis is from the neutron rich side, leaving the question of where the rare proton-rich stable isotopes which exist in nature are created, for they are impossible to create via neutron processes alone.

It is thought that supernovae type II, although responsible for the synthesis of most of the neutron rich isotopes and their distribution throughout the galaxies, are not responsible for the proton-rich rare isotopes. For these nuclides, a very high temperature hydrogen-rich environment would be required, leading into our consideration of stellar binary systems. p −process is aimed at

explaining the synthesis of the p-nuclei observed in the bulk solar system material. It could also provide some explanation for certain isotopic anomalies found in primitive meteorites, the p-nuclei cannot be produced by s- and r-processes of neutron captures. In contrast, it seems natural to think of the transformation of pre-existing seed nuclei (especially of the s- or r- type) by the addition of protons, or by removal of neutron.

The rates (γ, n) photodisintegrations are increasing very rapidly with increasing temperatures and decreasing neutron binding energies. It appears that temperatures $T \geq 10^9 K$ are required in order for s- or r-nuclei to have time to be stripped of neutrons in realistic stellar situations. On the other hand, (p, γ) reactions are much less dependent on temperature and binding energy, but their rates are rapidly decreasing with increasing Coulomb barrier heights. As a result, proton radiative captures can contribute at best to the production of the lightest p-nuclei production only, and in highly proton-rich environments.

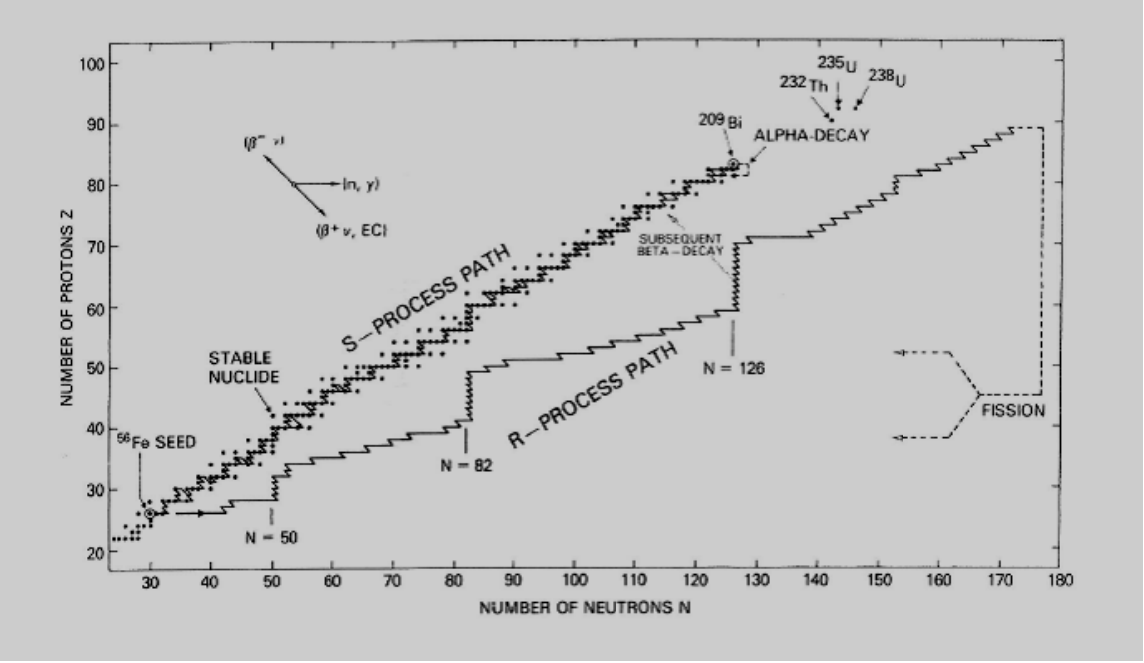

Fig 1.6. *The s,r and p neutron capture process.*

1.2.7. Spallation reaction:

It is the process in which a heavy nucleus emits a large number of nucleons as a result of being hit by a high-energy particle, thus greatly reducing its atomic weight. In the context of impact physics it describes ejection or vaporization of material from a target during impact by a projectile.

Spallation reactions take place in interstellar space when energetic ($\sim 10\ Mev$) cosmic rays (such as high-energy protons) collide with interstellar gas, which contains atoms such as carbon, nitrogen, and oxygen. This leads to the synthesis of light isotopes, such as ^{6}Li, ^{9}Be, ^{10}Be, and ^{11}B, that cannot be produced abundantly in nucleosynthesis scenarios in the big bang or stellar interiors. As example for this reaction is

$$^{12}C + p \rightarrow\ ^{7}Li + 2p + \alpha \tag{1.44}$$

1.3. Stellar evolution:

As it collapses, a molecular cloud breaks into smaller and smaller pieces. In each of these fragments, the collapsing gas releases gravitational potential energy as heat. As its temperature and pressure increase, the fragments condense into rotating spheres of gas. Once the gas is hot enough for the internal pressure to support the fragment against further gravitational collapse (hydrostatic equilibrium), the object is known as a protostar [Aud72].

Accretion of material onto the protostar continues partially through a circumstellar disc. When the density and temperature are high enough, deuterium fusion begins, and the outward pressure of the resultant radiation slows (but does not stop) the collapse. Material comprising the cloud continues to "rain" onto the protostar.

The protostar follows a Hayashi track on the Hertzsprung-Russell (H-R) diagram. The contraction will proceed until the Hayashi limit is reached, and thereafter contraction will continue with the temperature remaining stable. Stars with less than 0.5 solar masses thereafter join the main sequence. For more massive protostars, at the end of the Hayashi track they will slowly collapse in near hydrostatic equilibrium,

Finally, hydrogen begins to fuse in the core of the star, and the rest of the enveloping material is cleared away. This ends the protostellar phase and begins the star's main sequence phase on the H-R diagram. The later evolution of stars are studied in stellar evolution [Aud72]..

As the hydrogen around the core is consumed, the core absorbs the resulting helium, causing it to contract further, which in turn causes the remaining hydrogen to fuse even faster. This eventually leads to ignition of helium fusion (which includes the triple-alpha process) in the core. In stars of more than approximately 0.5 solar masses, electron degeneracy pressure may delay helium fusion for millions or tens of millions of years; in more massive stars, the combined weight of the helium core and the overlying layers means that such pressure is not sufficient to delay the process significantly.

When the temperature and pressure in the core become sufficient to ignite helium fusion in the core, a helium flash will occur if the core is largely supported by electron degeneracy pressure; in more massive stars, whose core is not overwhelmingly supported by electron degeneracy pressure, the ignition of helium fusion occurs relatively quietly. Even if a helium flash occurs, the time of very rapid energy release (on the order of 108 Suns) is brief, so that the visible outer layers of the star are relatively undisturbed. The energy released by helium fusion causes the core to expand, so that hydrogen fusion in the overlying layers slows, and thus total energy generation decreases. Therefore, the star contracts, although not all the way to the main sequence; it thus migrates to the horizontal branch on the HR-diagram, gradually shrinking in radius and increasing its surface temperature.

After the star has consumed the helium at the core, fusion continues in a shell around a hot core of carbon and oxygen. The star follows the Asymptotic Giant Branch on the HR-diagram, paralleling the original red giant evolution, but with even faster energy generation (which thus lasts for a shorter time) [Aud72].

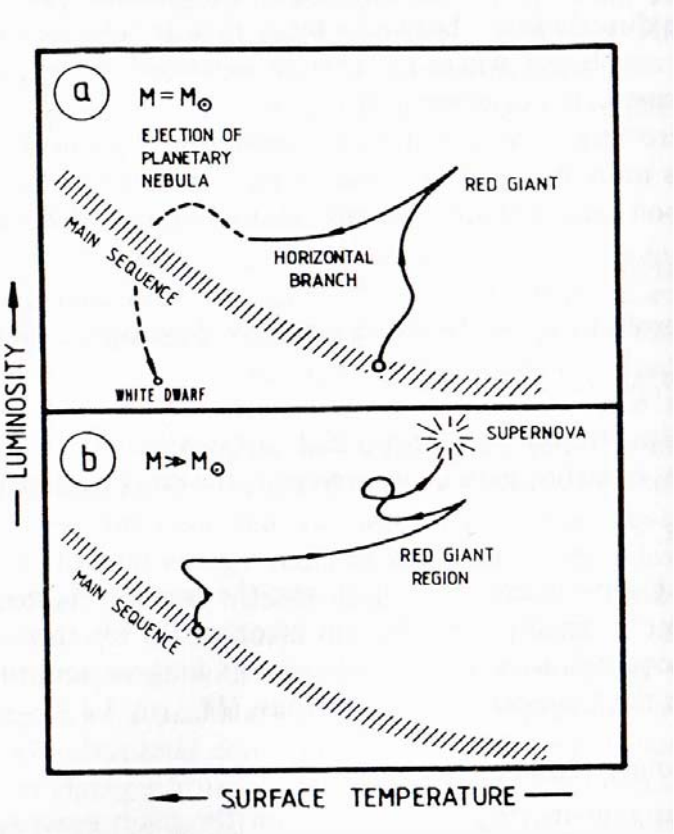

Fig 1.7. *Schematic and simplified diagram of the evolutionary track of a solar-mass star and a more massive.*

Changes in the energy output cause the star to change in size and temperature for certain periods. The energy output itself is shifted to lower frequency emission. This is accompanied by increased mass loss through powerful stellar winds and violent pulsations. Stars in this phase of life are called Late type stars, OH-IR stars or Mira-type stars, depending on their exact characteristics. The expelled gas is relatively rich in heavy elements created within the star, and may be particularly oxygen or carbon enriched depending on the type of the star. The gas builds up in an expanding shell called a circumstellar envelope and cools as it moves away from the star, allowing dust particles and molecules to form. With the high infrared energy input from the central star ideal conditions are formed in these circumstellar envelopes for maser excitation.

Helium burning reactions are extremely sensitive to temperature, which causes great instability. Huge pulsations build up, which eventually give the outer layers of the star enough kinetic energy to be ejected, potentially forming a planetary nebula. At the center of the nebula remains the core of the star, which cools down to become a small but dense white dwarf.

In massive stars, the core is already large enough at the onset of hydrogen shell burning that helium ignition will occur before electron degeneracy pressure has a chance to become prevalent. Thus, when these stars expand and cool, they do not brighten as much as lower mass stars; however, they were much brighter than lower mass stars to begin with, and are thus still brighter than the red giants formed from less massive stars. These stars are known as red supergiants.

Extremely massive stars (more than approximately 40 solar masses), which are very luminous and thus have very rapid stellar winds, lose mass so rapidly due to radiation pressure that they tend to strip off their own envelopes before they can expand to become red supergiants, and thus retain extremely high surface temperatures (and blue-white color) from their main sequence time onwards. Stars cannot be more than about 120 solar masses because the outer layers would be expelled by the extreme radiation. Although lower mass stars normally do not burn off their outer layers so rapidly, they can likewise avoid becoming red giants or red supergiants if they are in binary systems close enough so that the companion star strips off the envelope as it expands, or if they rotate rapidly enough so that convection extends all the way from the core to the surface, resulting in the absence of a separate core and envelope due to thorough mixing.

The core grows hotter and denser as it gains material from fusion of hydrogen at the base of the envelope. In a massive star, electron degeneracy pressure is insufficient to halt collapse by itself, so as each major element is consumed in the center, progressively heavier elements ignite, temporarily halting collapse. If the core of the star is not too massive (less than approximately 1.4 solar masses, taking into account mass loss that has occurred by this time), it may then form a white dwarf (possibly surrounded by a planetary nebula) as described above for less massive stars,

with the difference that the white dwarf is composed chiefly of oxygen, neon, and magnesium [Aud72].

The onion-like layers of a massive, evolved star just prior to core collapse. (Not to scale.). Above a certain mass (estimated at approximately 2.5 solar masses, within a star originally of around 10 solar masses), the core will reach the temperature (approximately 1.1 gigakelvins) at which neon partially breaks down to form oxygen and helium, the latter of which immediately fuses with some of the remaining neon to form magnesium; then oxygen fuses to form sulfur, silicon, and smaller amounts of other elements. Finally, the temperature gets high enough that any nucleus can be partially broken down, most commonly releasing an alpha particle (helium nucleus) which immediately fuses with another nucleus, so that several nuclei are effectively rearranged into a smaller number of heavier nuclei, with net release of energy because the addition of fragments to nuclei exceeds the energy required to break them off the parent nuclei.

A star with a core mass too great to form a white dwarf but insufficient to achieve sustained conversion of neon to oxygen and magnesium will undergo core collapse (due to electron capture, as described above) before achieving fusion of the heavier elements. Both heating and cooling caused by electron capture onto minor constituent elements (such as aluminum and sodium) prior to collapse may have a significant impact on total energy generation within the star shortly before collapse. This may produce a noticeable effect on the abundance of elements and isotopes ejected in the subsequent supernova.

For a star of 1 solar mass, the resulting white dwarf is of about 0.6 solar masses, compressed into approximately the volume of the Earth. White dwarfs are stable because the inward pull of gravity is balanced by the degeneracy pressure of the star's electrons.

If the mass of the stellar remnant is high enough, the neutron degeneracy pressure will be insufficient to prevent collapse below the Schwarzschild radius. The stellar remnant thus becomes a black hole. The mass at which this occurs is not known with certainty, but is currently estimated at between 2 and 3 solar masses.

CHAPTER 2

ASTROPHYSICAL NUCLEAR REACTIONS

2.1.Introduction

The thermonuclear reactions of astrophysical interest concern mainly the capture of nucleons or alpha particles. A limited number of fusion reactions involving heavy ions (^{12}C, ^{16}O) are also of great importance. Charged-particle induced reactions are essential for the energy budget of a star, as well as for the production of new nuclides in stellar and non-stellar (Big Bang) situations. In contrast, the role of neutron captures is largely restricted to nucleosynthesis, their energetic impact being negligible.

The heart of stellar evolution and nucleosynthesis is the thermonuclear reactions. It is the fusion of light nuclei into heavier nuclei that liberates kinetic energy (at the expense of mass) and serves as the interior source of the energy radiated from the surface. The condition that the power liberated internally balance the power radiated from the surface determines a steady state in the structure of the star. That situation cannot be a truly static one, however, because the very reactions that liberate energy necessarily change the chemical composition of the stellar interior. It is the slow change of chemical composition that causes the structure of the star to the chemical composition of the interstellar medium will have been altered by the thermonuclear debris. Stated most simply, it is the working hypothesis of the stellar nucleosynthesist that all or part of the heavy elements found in our galaxy have been synthesized in the interiors of stars by these same fusion reactions.

A complete science of thermonuclear reaction rates is formidable. It involves complicated details of nuclear physics, many of which are still unsolved. The mechanism of each reaction must be scrutinized to achieve assurance of the proper prescription for the stellar reaction rate. Still there are a few basic physical principles that are common to the computation of all thermonuclear reaction rates.

2.2. Kinematics and energetics

A nuclear reaction in which a particle *a* strikes a nucleus *X* producing a nucleus *Y* and a new particle *b* is symbolized by:

$$a + X \rightarrow Y + b \tag{2.1}$$

For example, a reaction in which a deuteron strikes a C^{12} nucleus producing a nucleus and a proton is written:

$$d + C^{12} \rightarrow C^{13} + p \tag{2.2}$$

An alternative notation in common usage is

$$X(a,b)Y \equiv C^{12}(d,p)C^{13}. \tag{2.3}$$

In all such nuclear reactions, the total energy, momentum and angular momentum are conserved quantities.

For two particles of masses m_1 and m_2, and non-relativistic velocities v_1, v_2, the velocity V of the center of mass is given by the value of the momentum:

$$m_1\overrightarrow{v_1} + m_2\overrightarrow{v_2} = (m_1 + m_2)\vec{V} \tag{2.4}$$

Or

$$\vec{V} = \frac{m_1\overrightarrow{v_1} + m_2\overrightarrow{v_2}}{(m_1+m_2)} \tag{2.5}$$

This discussion will be entirely restricted to the non-relativistic kinematics appropriate to the low kinetic energy in stellar interiors [Cla86].

The momentum of particle 1 relative to the center of mass is

$$m_1\left(\overrightarrow{v_1} - \vec{V}\right) = \frac{m_1 m_2}{m_1+m_2}(\overrightarrow{v_1} - \overrightarrow{v_2}) = \mu\vec{v} \tag{2.6}$$

where μ is the reduced mass

$$\mu = \frac{m_1 m_2}{m_1+m_2} \tag{2.7}$$

And $\vec{v}$ is the relative velocity of m_1 and m_2

$$\vec{v} = (\overrightarrow{v_1} - \overrightarrow{v_2}) \tag{2.8}$$

In the same manner the momentum of m_2 relative to the center of mass is

$$m_2\left(\overrightarrow{v_2} - \vec{V}\right) = -\mu\vec{v} \tag{2.9}$$

The kinetic energy before the collision is

$$(KE)_i = \frac{1}{2}m_1v_1^2 + \frac{1}{2}m_2v_2^2 \tag{2.10}$$

Or

$$(KE)_i = \frac{1}{2}(m_1 + m_2)V^2 + \frac{1}{2}\mu v^2 \tag{2.11}$$

Equation (2.11) indicates that the kinetic energy of two particles can be thought of as the sum of those associated with a mass $m_1 + m_2$, moving with the velocity of the center of mass plus a mass μ moving with the relative velocity $\vec{v}$. The first term is the kinetic energy of the center of mass itself, which must be the same after the collision as before it. The second term, $\frac{1}{2}\mu v^2$, represents that portion of the kinetic energy available for doing work against any force separating the two particles. It is commonly called the kinetic energy in the center- of – mass system.

These non-relativistic formulas are applicable to nuclear reactions only if the combined mass of the final particles equals the combined mass of the initial particles. But the source of new kinetic energy comes from a reduction of mass according to the Einstein relationship

$$\Delta KE = -\Delta Mc^2 \tag{2.12}$$

In low energy nuclear reactions, however, $\Delta M/M \approx 10^{-2} \rightarrow 10^{-4}$ so that that assumption of constant mass is accurate to better than 0.1 percent. For our purposes it is adequate to consider that to equality. Since the kinetic energy of the center of mass is accordingly unchanged by the reaction, the kinetic energy in the center-of-mass system must be increased or decreased according to whether the final mass is less than or greater than the initial mass.

Thus if we return to the reaction

$$a + X \rightarrow Y + b$$

the conservation of energy principle demands the equality

$$E_{aX} + (M_a + M_X)c^2 = E_{bY} + (M_b + M_Y)c^2 \quad (2.13)$$

where E_{aX} is the center-of-mass kinetic energy of a and X and E_{bY} is the kinetic energy in the center of mass of the bY system. The second terms on each side of the equation represent the fact that the sums of the rest masses before and after the reaction are not necessarily exactly equal and that kinetic energy may be either liberated or absorbed by that inequality. This is the well-known Einstein mass-energy relationship. The masses involved are the masses of the nuclei *a ,X; b,* and *Y.*
Another quantity that is clearly equal on both sides of the nuclear-reaction equation is the total number of nucleons (nucleon is the generic name of a neutron or a proton). Hence the atomic weight, which is defined as the integer nearest in value to the exact mass expressed in atomic mass units, remains the same on both sides of the mass-energy equation. The energy balance itself is not disturbed, therefore, by subtracting the atomic weight times the rest-mass energy of 1 amu from both sides of the equation. The masses then become the excesses of mass over integral number of atomic mass units. We define the atomic mass excess in units of energy by the quantity

$$\Delta M_{AZ} = (M_{AZ} - AM_u)c^2 \quad (2.14)$$

$$\Delta M_{AZ} = [M_{AZ}(amu) - A]c^2 M_u \quad (2.15)$$

Where M_u is the mass of 1 atomic mass unit (amu), defined as one-twelfth of the mass of the neutral atom. In the convenient numerical units of Mev

$$\Delta M_{AZ} = 931.478(M_{AZ} - A) \quad Mev \quad (2.16)$$

Where 931.478 is the rest mass energy of 1 amu in Mev and M_{AZ} is the mass of species *(A,Z)* in atomic mass units. With this definition the energy-balance equation becomes

$$E_{aX} + (\Delta M_a + \Delta M_X) = E_{bY} + (\Delta M_b + \Delta M_Y) \quad (2.17)$$

where ΔM Are expressed in energy units, generally in Mev.

2.3. Reaction rate

Let us consider a hot ionized gas containing nuclei of type A and B, with concentrations N_A and N_B which can fuse with a fusion cross section denoted by σ, both types of nuclei move and the fusion cross section depends on the relative speed v_r of the nuclei. If $P(v_r)dv_r$ denotes the probability that the relative speed is between v_r and $v_r + dv_r$, then the average value of the product of the fusion cross section and the relative speed is

$$\langle \sigma v_r \rangle = \int_0^\infty \sigma v_r P(v_r) dv_r \tag{2.18}$$

The mean time for a nucleus A to fuse with B nucleus is given by [Phi94]

$$\tau_A = \frac{1}{N_B \langle \sigma v_r \rangle} \tag{2.19}$$

and the A-B fusion rate per unit volume can be written:

$$R_{AB} = N_A N_B \langle \sigma v_r \rangle \tag{2.20}$$

In most astrophysical situations the nuclei form a classical, non relativistic gas with a speed distribution given by the Maxwell-Boltzmann distribution.

$$P(v_r)dv_r = \left[\frac{\mu_r}{2\pi KT}\right]^{3/2} exp\left[\frac{m_r v_r^2}{2KT}\right] 4\pi v_r^2 dv_r \tag{2.21}$$

The average value of the product of the fusion cross section and the relative speed can be calculated using (2.21)

$$\langle \sigma v_r \rangle = \left[\frac{8}{\pi m_r}\right]^{0.5} \left[\frac{1}{KT}\right]^{3/2} \int_0^\infty E\sigma(E) exp\left[\frac{-E}{KT}\right] dE \tag{2.22}$$

2.4. The cross section:

The cross section $\sigma(E)$ is the product of these terms:

$$\sigma(E) = \sigma_1 . P . C \tag{2.23}$$

where

$$\sigma_1 = \pi\lambda_\beta^2 = \frac{\pi h^2}{2\mu E} \tag{2.24}$$

The important functions P is the penetration probability (factor) of the potential barrier-see Fig(2.1)-.

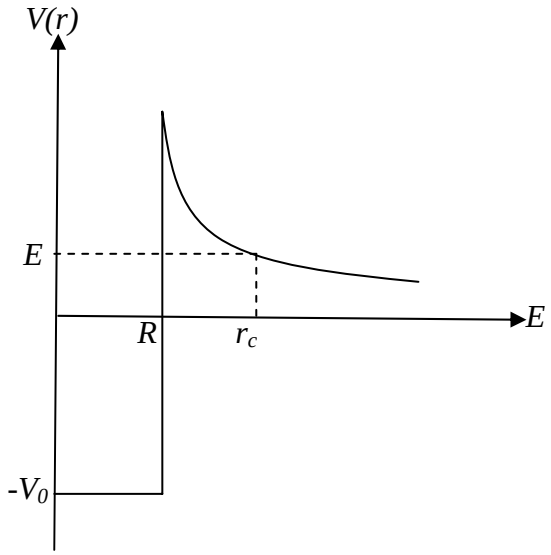

Fig.2.1 *A representation of the Coulomb potential*.

It is obtained by solving the Schrödinger radial equation

$$\frac{d^2X}{dr^2} + \frac{8\pi^2}{h^2}(E - V)X = 0 \tag{2.25}$$

where

$$V(r) = \begin{cases} \frac{Z_1 Z_2 e^2}{r} & for\ r > R \\ -V_0 & for\ r < R \end{cases} \tag{2.26}$$

The penetration factor is then obtained as

$$P = exp\left[-\frac{4\pi(2\mu)^{0.5}}{\hbar}\int_R^{r_c}\sqrt{V - E}\,dr\right] \tag{2.27}$$

This expression can be reduced to the approximate one

$$P = e^{\left(-\frac{E_G}{E}\right)^{1/2}} \tag{2.28}$$

E_G is called Gamow energy. It is given by

$$E_G = \frac{8\pi^4 \mu}{h^2} Z_1^2 Z_2^2 e^4 \tag{2.29}$$

The C term is the probability that the considered reaction occurs effectively after barrier penetration for non resonant reaction C is almost energy independent.

The reaction rates can then written as:

$$R_{AB} = \frac{\sqrt{2}}{(\mu KT)^{3/2}} C N_A N_B \int_0^\infty exp\left[\frac{-E}{KT} - \left(\frac{E_G}{E}\right)^{1/2}\right] dE \tag{2.30}$$

The expression in the integral is the product of the Maxwell terme exp $(\frac{-E}{KT})$ and the Gamow term $exp\left(\frac{E_G}{E}\right)^{1/2}$. This product shows a relatively narrow maximum called *Gamow pic* – see Fig2.2.-.

The integral can be evaluated approximately to get the reaction rate:

$$R_{AB} = \frac{4h^2 N_1 N_2}{\mu^{\frac{3}{2}} (KT)^{2/3}} C {E_G}^{1/6} \exp\left[-1.89\left(\frac{E_G}{E}\right)^{1/3}\right] \tag{2.31}$$

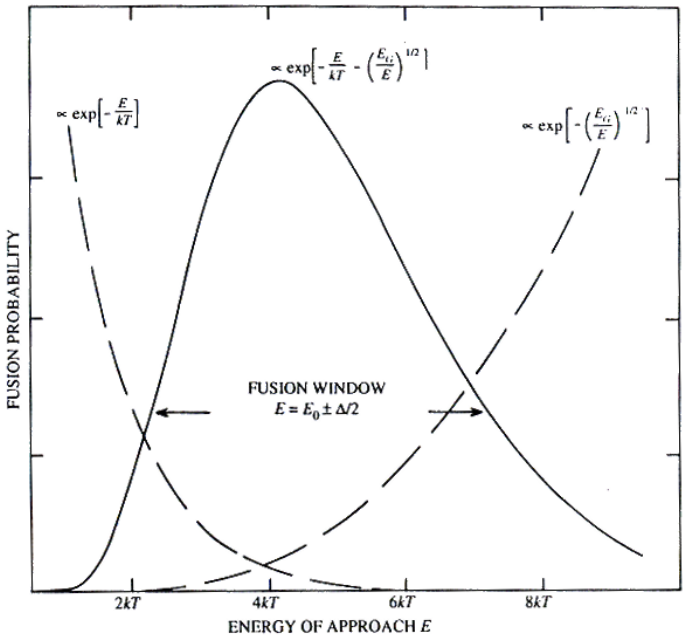

Fig 2.2 . *The energy window for the fusion of nuclei with Gamow energy E_G and temperature* T.

2.5. The astrophysical factor

In order to extrapolate measured nuclear cross section $\sigma(E)$ down to astrophysical energies, the nuclear cross section factor $S(E)$ is introduced by

$$\sigma(E) = \frac{S(E)}{E}\exp(-2\pi\eta) \tag{2.32}$$

Where η is the Sommerfield parameter

$$\eta = \frac{Z_1 Z_2 e^2}{\hbar v} = \frac{\mu^{\frac{1}{2}}}{2}.\frac{Z_1 Z_2 e^2}{\hbar E^{1/2}} \tag{2.33}$$

With Z being the atomic charge and *v* the asymptotic relative velocity of the reacting nuclei. As already mentioned (section 2.3), the cross section is given by the product of the cross section factor to be determined experimentally, the square of the De Broglie wavelength due to quantum mechanics ($\approx E^{-1}$) and the barrier penetration factor. The quantity $\exp(-2\pi\eta)$ takes exclusively s-wave transmission into account, describing penetration to the origin through a pure Coulomb

potential. Nuclear reaction rates are extremely sensitive to the precise numerical value in the argument of this exponential factor. The inclusion of uncertainties in the shape of the nuclear potential and contributions from non s-wave transmission, respectively are very important for deriving nuclear reaction rates but do not change the overall energy dependence of the nuclear cross section given in (2.32). Actually, uncertainties in the shape of the nuclear potential tail and contributions from non s-wave terms are only important for heavy ion reactions. The main uncertainty in (2.32) lies in the variation of the cross section factor $S(E)$ with energy, which depends primarily on the value chosen for the radius at which formation of a compound nucleus between two interacting nucleons occurs.

The separation of the barrier penetration factor in (2.32) is based on the solution of the Schrödinger equation for the Coulomb wave function. Therefore, the cross section $\sigma(E)$ in (2.32) can be parameterized even more precisely by either expanding $S(E)$ into a Taylor series about zero energy because of its slow energy dependence

$$S(E) = S(0)\left[1 + \frac{S'(0)}{S(0)}E + 0.5\frac{S''(0)}{S(0)}E^2\right] \tag{2.34}$$

Where $S(0)$ is the value of *S(E)* at zero energy and $S'(0)$ and $S''(0)$ are the first and second derivatives of *S(E)* with respect to energy evaluated at *E*=0, respectively.

CHAPTER 3

ATOMIC SCREENIG IN ASTROPHYSICAL NUCLEAR REACTIONS

3.1. Electron screening effects in low energy reactions:

3.1.1. Introduction

At very low energy, the cross section of nuclear reactions induced by charged particles decreases drastically due to the steep drop in the Coulomb penetration and the geometrical factor $\pi\lambda^2 \sim 1/E$. In various applications it is advantageous to remove this strong energy dependence and an astrophysical $S(E)$ factor is defined [Cla86]:

$$S(E) = \sigma(E)Eexp(2\pi\eta) \tag{3.1}$$

Where $\sigma(E)$ is the nuclear reaction cross and $\eta = Z_1 Z_2 e^2/\hbar v$ denotes the usual Coulomb parameter for nuclei with charge number $Z_1$and Z_2 in the entrance channel, respectively. If no resonant effects are present the $S(E)$ factor varies slowly with energy and also allows for the extrapolation of data to zero energy [Cla86].

Usually, in the treatment of nuclear reactions, atomic and molecular effects are ignored so that the cross section contains only the effect of the Coulomb repulsion and nuclear attraction between bare nuclei. However, in the actual experiments target nuclei are in the form of atoms or molecules and electronic screening effects reduce the Coulomb repulsion and, hence, the cross section of the various processes will be affected.

Electron screening effects may be especially crucial in some fusion reactions of astrophysical importance at very low energies. Assenbaum, Langanke and Rolfs [Ass87] have studied nuclear fusion reactions and found that a significant enhancement of the cross section can occur at energies which are about a hundred times larger than the electron binding energies involved. Thus, screening effects must be well understood in order to interpret and extrapolate nuclear reaction data to astrophysical energies.

While low energy fusion reactions were extensively studied, the effects of electron screening have been directly observed for the first time only by Engstler [Eng88], a nearly exponential enhancement of the $S(E)$ factor has been found at energies below $10\ keV$. The result

could be interpreted in terms of a simple astrophysical screening model although the agreement with experimental data below 10 keV needs improvement. The experimental data on $S(E)$, as well as the bare nucleus value obtained from a polynomial fit to higher energy data, are displayed on figures 3.1 and 3.2 for the $^3He(d,p)^4He$ and $d(^3He,p)^4He$ reactions, respectively. In the latter case the enhancement is smaller due to the molecular nature of the D_2 target.

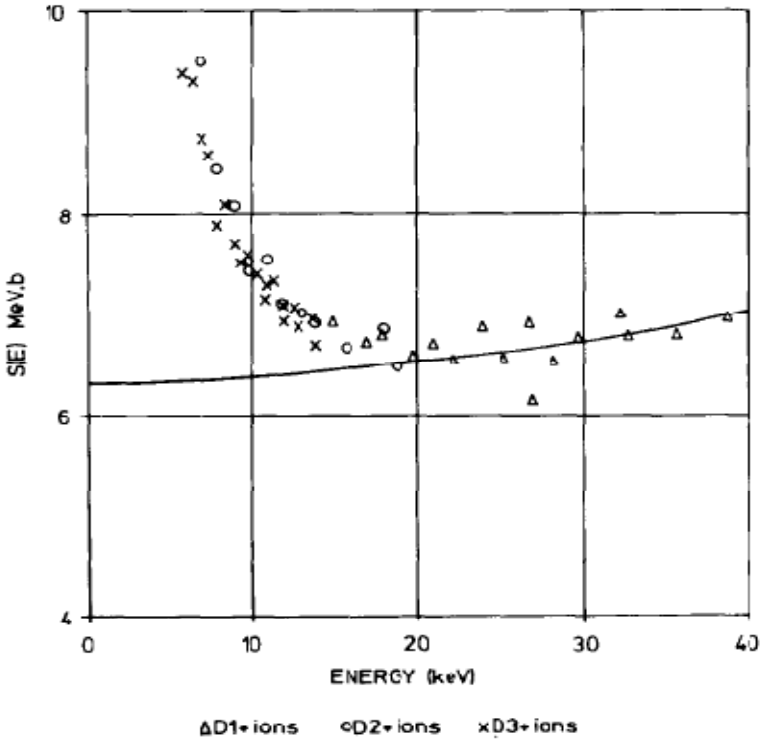

Fig 3.1. $S(E)$ for the $^3He(d,p)^4He$. The solid line represents the bare nucleus value taken from[Eng88]

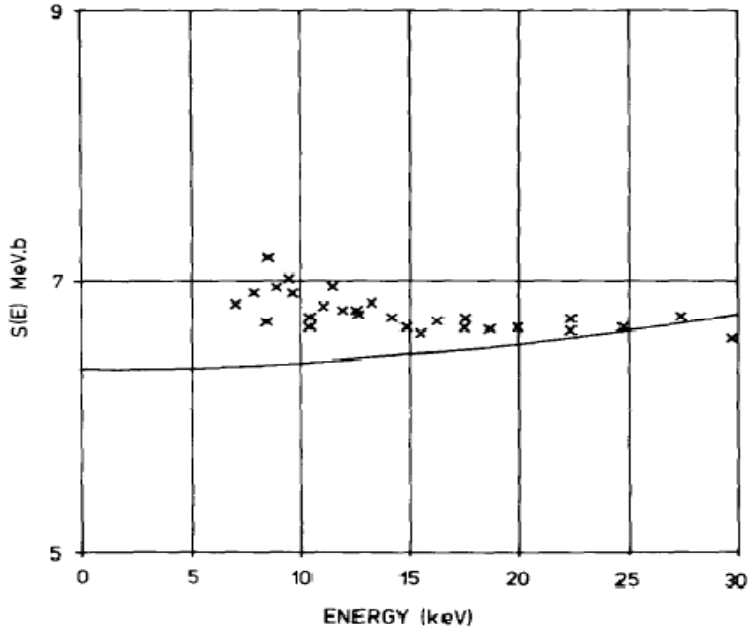

Fig 3.2: $S(E)$ for the$d(^3He,p)^4He$. The solid line represents the bare nucleus value taken from [Eng88]

In this section we introduce the models describing the electron screening effects that appear in laboratory nuclear reactions at astrophysical energies for the screening. The only parameter is the screening radius, which for the electronic density and the corresponding screening potential can be determined by more sophisticated considerations like in [Strl01].

3.2. Coulomb screened potential

3.2.1. Prior work:

The screening enhancement effect in laboratory nuclear reactions at astrophysical energies has attracted a lot of attention. The very low energies attained for the break up reaction $^3He(^3He, 2p)^4He$ [Ass87] which is extremely important to the solar neutrino production, revealed the real magnitude of the problem, as the screening energy obtained in that experiment still exceeds all available theoretical predictions. Other low energy experiments of the proton-proton chain still need a theoretical model that could account for the observed enhancement [Lio01].

Various theoretical models have been proposed, some of which are in conflict with each other (ref [Eng98] or [Lan96]) while others [Ben89] were applied at a time when experimental measurements [Kra87a] were too scarce and inaccurate, thus their actual validity has been obscured.

After the pioneering work [Ass87] that established the importance of atomic effects in low energy nuclear reactions, various authors have tried to create models that account for the observed enhancement. A simple model [Ben89], suggested at an early stage, assumed that the electronic charge density around the target nucleus is constant, thus predicting for the nucleus-atom reaction between the atomic target $Z_1 e$ and the projectile $Z_2 e$ a screening energy $U_e = \left(\frac{3}{2}\right) Z_1 Z_2 e^2 a^{-1}$, that model used a screening radius taken from scattering experiments so that

$$a = 0.8855 a_0 \left(Z_1^{2/3} + Z_2^{2/3}\right)^{-1/2} \tag{3.2}$$

where $a_0 = 0.529A°$ is the Bohr radius. Although that screening energy is larger than the one predicted by the simple formula $U_e = Z_1 Z_2 e^2 \left(\frac{a_1}{Z_1}\right)^{-1}$, it has some very obvious defects. The assumption that the charge density is constant leads to an unnaturally sharp cut-off at a distance $r = a$ from the center of the target nucleus. Moreover, atomic excitations and deformations of the

target atom are totally discarded. On the other hand normalizing the charge distribution so that the total charge is $-Z_1 e$ gives a charge density

$$\rho_0 = -\frac{3}{4}\frac{Z_1 e}{\pi a^3}. \tag{3.3}$$

Liolios, in his work [Lio00], proposed a simple and efficient model for the study of the screening enhancement effect on low energy nuclear fusion reaction. In that model the fusing atoms are considered as Hydrogen-like atoms whose electron probability density is used in Poisson's equation in order to derive the corresponding screened coulomb potential energy

As a first step he considers a charge distribution Fig.3.3:

$$\rho(r) = \rho_0 \left(1 - \frac{r^2}{a^2}\right). \tag{3.4}$$

which takes into account the depletion of charge with respect to distance from the center. The radius a is the screening radius given by equation (3.2) and the charge density ρ_0 at the center of the cloud can be found by means of the normalization condition:

$$\int_0^a \rho(r) 4\pi r^2 dr = -Z_1 e \tag{3.5}$$

This integral yields a central value of

$$\rho_0 = -\frac{15}{8}\frac{Z_1 e}{\pi . a^3} \tag{3.6}$$

Note that for a collision $Z_1 = Z_2 = 1$ we have a central density $\rho_0 = 7.68(e/a_0^3)/\pi$ which gives an even larger density than the constant density assumption. An alternative approach would be to consider the value ρ_0 equal to the corresponding hydrogen-like one and then calculate the screening radius using equation (3.5) the latter treatment gives a screening radius

$$a = \left(\frac{15}{8Z_1^2\pi}\right)^{1/3} a_0. \tag{3.7}$$

which is independent of the charge of the projectile. For hydrogen isotopes equation (3.7) gives a radius of $a = 0.842a_0$

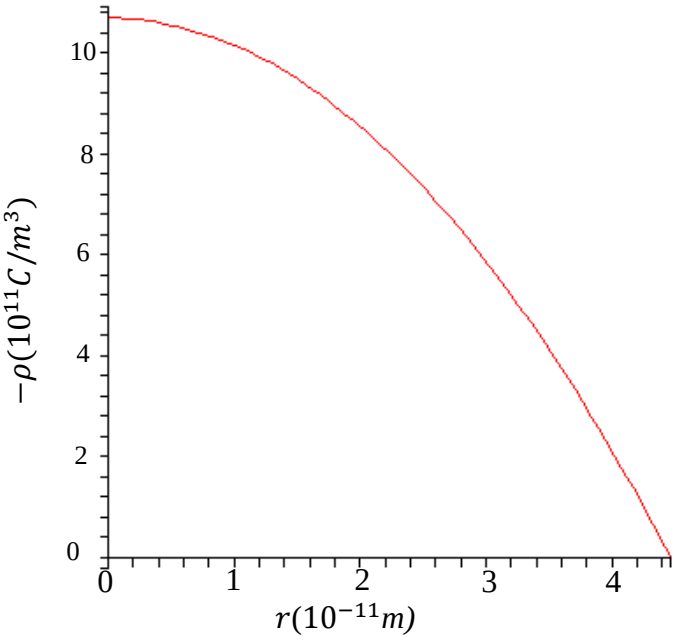

Fig3.3. *Liolios's charge distribution*

The electrostatic energy is calculated by solving the equation of Poisson for the above charge distribution with the appropriate boundary condition: $\Phi(\infty) = 0$, $\Phi(r \to 0) = \frac{Z_1 e}{r}$ so that

$$\Phi(r) = -\frac{15}{12}\frac{Z_1 e}{a}\left[\frac{3}{2} - \left(\frac{r}{a}\right)^2 + \frac{3}{10}\left(\frac{r}{a}\right)^4\right] \tag{3.8}$$

Whenever a bare nucleus $Z_1 e$ impinges on the target nuclei surrounded by the electron cloud of equation (3.4) the total interaction potential in the atom-nucleus reaction channel is

$$V(r) = \frac{Z_1 Z_2 e^2}{r} - \frac{15}{12}\frac{Z_1 Z_2 e^2}{a}\left[\frac{3}{2} - \left(\frac{r}{a}\right)^2 + \frac{3}{10}\left(\frac{r}{a}\right)^4\right] \tag{3.9}$$

3.2.2. BES model (Batna Electron Screening Model)

In the model, which was proposed by Liolios, the density of electrons decreases rapidly as a function of distance and shows a sudden cut off for $r = a$, which is not in agreement with the

quantum description. In order to get a gradual decreasing of charge density we have proposed the following form of the charge density (Fig.3.4):

$$\rho(r) = \rho_0 exp\left(-\frac{r^2}{a^2}\right). \tag{3.10}$$

where ρ_0 is charge density at the center of the cloud (when the electron is in its ground state)

$$\rho_0 = -\frac{e\left(\frac{Z_1}{a_0}\right)^3}{\pi}. \tag{3.11}$$

From the condition of normalization

$$\int_0^a \rho(r) 4\pi r^2 dr = -Z_1 e$$

the screening radius is obtained as a function of ρ_0:

$$\rho_0 = -\frac{Z_1 e}{2.379 a^3} \tag{3.12}$$

Using (3.11) one gets for $Z_1 = 1$:

$$a = 1.09418\, a_0 \tag{3.13}$$

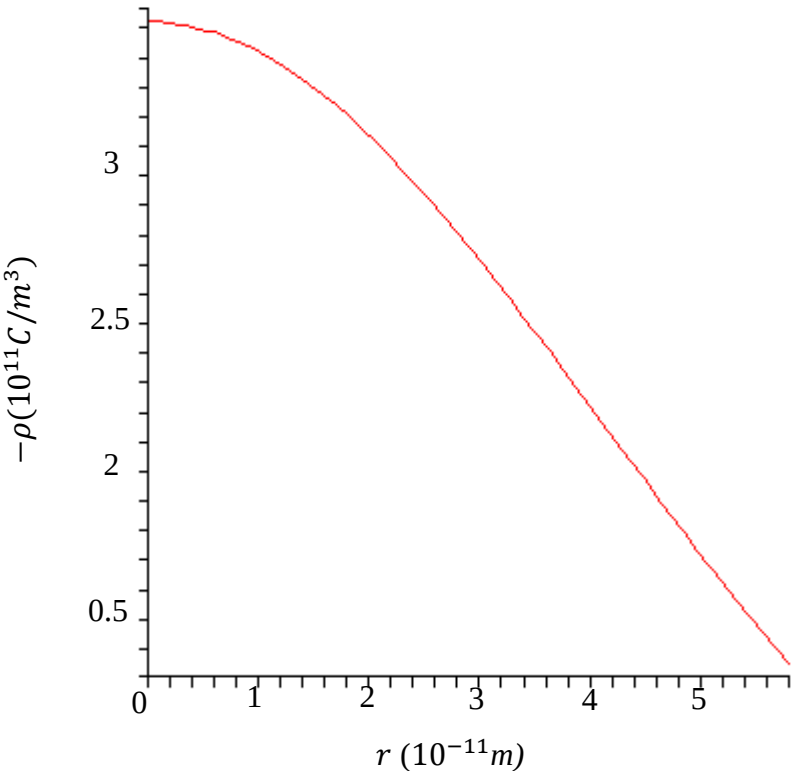

Fig3.4 *Charge distribution in the BES model*

The electrostatic potential of the distribution is given by the solution of Poisson's equation

$$\frac{1}{r^2}\frac{d}{dr}\left(r^2\frac{d\Phi(r)}{dr}\right) = -4\pi\,\rho_0 exp(-\frac{r^2}{a^2}) \tag{3.14}$$

Upon integration, we obtain:

$$\Phi(r) = \frac{4\pi\,\rho_0}{4}\frac{a^3}{r}\sqrt{\pi}Erf[\frac{r}{a}] \tag{3.15}$$

with

$$\rho_0 = -\frac{Z_1 e}{2.379a^3}$$

The projectile-target potential energies then

$$V(r) = \frac{Z_1 Z_2 e^2}{r} - \frac{Z_2 Z_1 e^2}{2.379r}\pi^{3/2}Erf[\frac{r}{a}] \tag{3.16}$$

3.2.3. Comparison with Liolios Model:

The charge radius obtained in our work (3.13) is greater than the one obtained by Liolios (3.7).

The comparison between Liolios's and BES's for the charge density calculation is shown schematically in Fig 3.5

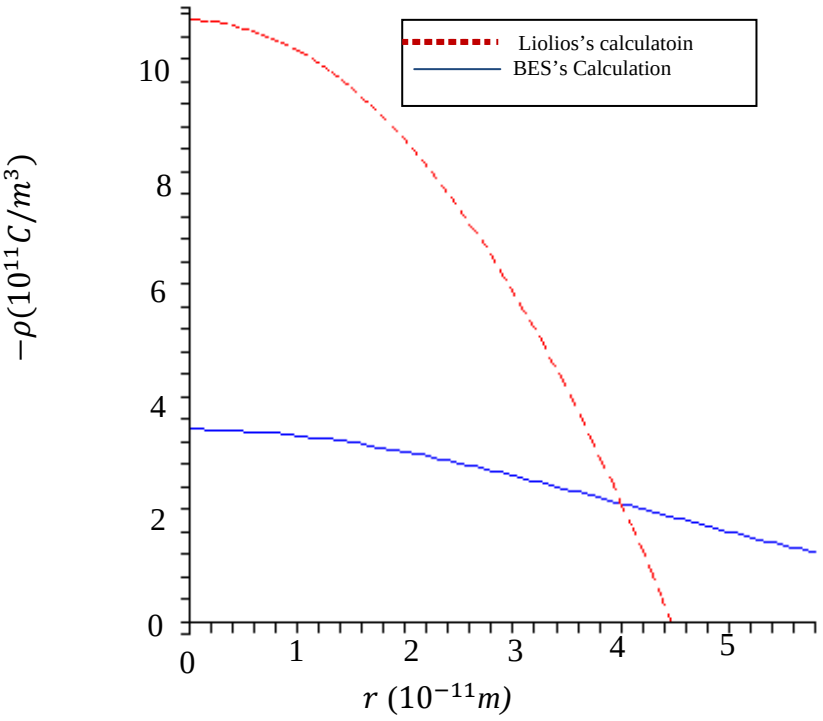

Fig 3.5: *Comparison between Liolios's and BES's charge density*

However, since the two approaches are slightly different, a strait forward comparison is obtained if one starts with the same input (3.2). Using (3.12), we obtain (for $Z_1 = Z_2 = 1$)

Finally we obtain

$$\rho_0 = \frac{-e}{0.626 a_0^3}$$

which is 50% less than the central density given by (3.6). Let $\rho_0^0 = -\frac{e}{a_0^3}$, so we obtain

$$\begin{cases} \rho^{BES} = 1.7123 exp\left(-\frac{r^2}{a^2}\right) \\ \rho^{Lio} = 2.9945 \rho_0^0 \left(1 - \frac{r^2}{a^2}\right) \end{cases} \tag{3.17}$$

Fig.3.6 shows a comparison between the two densities with the same parameterization (3.2).

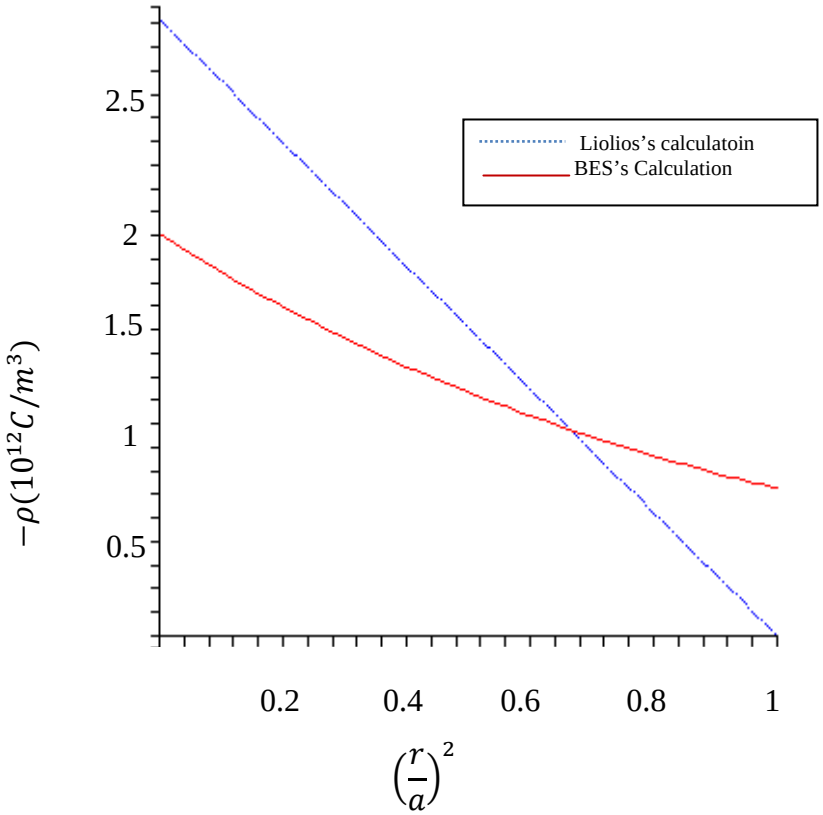

Fig 3.6: *Comparison between Liolios's and BES's charge densities with the same charge and radius a*

Let us now compare the potential energy in the two models.

The Taylor series for the error function is as follows:

$$Erf\left(\frac{r}{a}\right) = \frac{2}{\sqrt{\pi}}\left(\frac{r}{a} - \frac{1}{3}\frac{r^3}{a^3} + \frac{1}{10}\frac{r^5}{a^5} - \frac{1}{42}\frac{r^7}{a^7} + \frac{1}{216}\frac{r^9}{a^9} - \cdots\right) \tag{3.18}$$

We substitute equation (3.18) with the value of ρ_0 in equation (3.15) we obtain

$$\Phi(r) = \frac{-z_1 e}{2.379}[1 - \frac{1}{3}\left(\frac{r}{a}\right)^2 + \frac{1}{10}\left(\frac{r}{a}\right)^4 - \frac{1}{42}\left(\frac{r}{a}\right)^6 + \frac{1}{216}\left(\frac{r}{a}\right)^8] \tag{3.19}$$

The total interaction potential in the aotm-nucleus reaction channel is

$$V(r) = \frac{Z_1 Z_2 e^2}{r} - \frac{Z_1 Z_2 e^2}{2.379a}\left[1 - \frac{1}{3}\left(\frac{r}{a}\right)^2 + \frac{1}{10}\left(\frac{r}{a}\right)^4 - \frac{1}{42}\left(\frac{r}{a}\right)^6 + \frac{1}{216}\left(\frac{r}{a}\right)^8\right] \tag{3.20}$$

We make a comparison between the equations (3.20) and (3.9) and we find that there are terms of the order higher then 4; therefore, they are considered as the terms of corrections.

If we write, equation (3.9) and (3.20) as a function of a, we have:

$$V^{BES}(r) = \frac{Z_1 Z_2 e^2}{r} - \frac{6}{50}\frac{Z_1 Z_2 e^2}{a_0}\left[1 - \frac{4}{5}\left(\frac{r}{a_0}\right)^2 + \frac{21}{100}\left(\frac{r}{a_0}\right)^4 - \frac{1}{20}\left(\frac{r}{a_0}\right)^6 + \frac{1}{144}\left(\frac{r}{a_0}\right)^8\right] \tag{3.21}$$

$$V^{Lio}(r) = \frac{Z_1 Z_2 e^2}{r} - \frac{2\,Z_1 Z_2 e^2}{a_0}\left[\frac{3}{2} - \frac{5}{2}\left(\frac{r}{a_0}\right)^2 + \frac{39}{20}\left(\frac{r}{a_0}\right)^4\right] \tag{3.22}$$

We remark that there is a difference between the terms in the two formulae. This is due to the difference in a radius and density.

3.3. One electron Screening effects:

Now consider a hydrogen-like atom with atomic number Z_1. When the wave function of the electron is given by $\Psi_{nl}(r,\theta)$ then the charge density around the point- like nucleus is

$$\rho_{nl}(r,\theta) = -e\left|\Psi_{nl}(r,\theta\right|^2 . \tag{3.23}$$

Assuming spherically symmetric wave functions for simplicity, we can solve the equation of Poisson for the above charge density in order to derive a screened Coulomb potential $\Phi(r)$ around the nucleus. Note that this potential will take into account the repulsive effects of the point-like nucleus, by imposing the appropriate boundary conditions $\Phi(\infty) = 0$, $\Phi(0) = \frac{Z_1 e}{r}$

The second boundary condition indicates that if a positive projectile (Z_2e) is in contact with the nucleus (Z_1e) at the center of the electron cloud, then there is no negative charge between them to reduce the Coulomb barrier.

The Poisson's equation for hydrogen atoms whose electron is in its ground state (1s) is:

$$\frac{1}{r^2}\frac{d}{dr}\left(r^2\frac{d\Phi(r)}{dr}\right) = -4\pi\,\rho_0 \exp\left(-\frac{r}{r_0}\right) \tag{3.24}$$

Where $\rho_0 = \frac{-e}{\pi}\left(\frac{Z_1}{a_0}\right)^3$ the charge density at the center of the electron cloud, and $r_0 = \frac{a_0}{2Z_1}$ is the screening radius [Lio01].

So we obtain :

$$\Phi_{00}(\mathrm{r}) = -\frac{\mathrm{C}_2}{\mathrm{r}} + \mathrm{C}_1 - 4\pi\rho_0 {r_0}^2\left(1+\frac{r}{2r_0}\right)exp\left(-\frac{r}{r_0}\right) \tag{3.25}$$

The electrostatic potential $\Phi_{00}(\mathrm{r})$ must go to zero at infinity which gives $C_1 = 0$. At very large distances $r \gg r_0$, due to the spherical symmetry of the distribution, any projectile impinging on that cloud will actually "see" a Coulomb potential of the form [Lio01]

$$\Phi_e(r \gg r_0) = -\frac{e}{r} \tag{2.26}$$

so that $C_2 = -e$. Inserting the values of the parameters r_0 and $\rho(0)$ into the above equation we obtain the formula used without details of its derivation

$$\Phi_{00}(\mathrm{r}) = -\frac{\mathrm{e}}{\mathrm{r}} + \frac{\mathrm{e}}{\mathrm{r}}\left(1+\frac{r}{2r_0}\right)exp\left(-\frac{r}{r_0}\right) \tag{3.27}$$

Then the total potential energy is:

$$V_{00} = \frac{Z_1Z_2e^2}{r} - \frac{\mathrm{Z_2e^2}}{\mathrm{r}} + \frac{Z_2\mathrm{e}^2}{\mathrm{r}}\left(1+\frac{r}{2r_0}\right)exp\left(-\frac{r}{r_0}\right) \tag{3.28}$$

If we assume that the electron is in an excited state (2s) then the potential energy is found to be:

$$V_{10} = \frac{Z_1 Z_2 e^2}{r} - \frac{Z_2 e^2}{r} + \frac{Z_2 e^2}{r}\left(1 + \frac{3r}{8r_0} + \frac{r^2}{16r_0^2} + \frac{r^3}{64r_0^3}\right) exp\left(-\frac{r}{r_0}\right) \quad (3.29)$$

If a positive projectile $Z_2 e$ impinges onto the above hydrogen like atom the total potential energy *V(r)* between the two nuclei will be due to the above electrostatic potential, that is $Z_2 e\Phi_e$, plus the repulsive potential of the nucleus $Z_1 e$:

$$V_{SC} = \frac{Z_1 Z_2 e^2}{r} - \frac{Z_2 e^2}{r} + \frac{Z_2 e^2}{r}(1 + \frac{r}{2r_0^*}) \exp(r / r_0^*) \quad (3.30)$$

Where

$$r_0^* = \frac{a_0}{2(Z_1 + Z_2)} \quad (3.31)$$

The reason for replacing r_0 with r_0^* is that, at astrophysical energies, the electrons move at higher velocities than the nuclei themselves [Lio01]. For example in laboratory *d-D* reactions the relative nuclear velocity equals the typical electron velocity $v_e = \alpha.c$ for $E = 25keV$. Although the above assumption is particularly valid at such low energy collisions between hydrogen nuclei, when reactions between heavier nuclei are considered an inevitable small error is involved at intermediate energies. The WKB treatment of the penetration factor disregards all effects beyond the classical turning point. Therefore, inside the tunnelling region, the wave function of the electron actually corresponds to a combined nuclear molecule ($Z_1 + Z_2$) instead of the initial Z_1 atom. Of course, this is an approximation.

3.4.Two electron screening effects:

Let us now assume that a Hydrogen-like atom $Z_2 e$ impinges on a resting target nucleus $Z_1 e$. Let us assume that the target atom has two electrons orbiting the nucleus [Lio01]. In a Hartree-Fock approximation the total potential energy of interaction will be:

$$V_{sc} = V_c(r) + V_{n_2 e_1}(r) + V_{n_2 e_2}(r) + V_{n_1 e}(r) + V_{e_1 e_2}(r) + V_{e_1 e}(r) + V_{e_2 e}(r) \quad (3.32)$$

That is the sum of : a) the Coulomb potential energy $V_c(r)$ between the two bare nuclei plus b) the interaction between the projectile (n_2) and the electrons $(e_{1,2})$ of the target nucleus, plus c) the interaction between the target nucleus (n_1) and the electron of the projectile (e), plus d) the interaction between the electrons of the target $V_{e_1e_2}(r)$ and of course, the interaction (e_1e, e_2e) between the electron of the projectile and those of the target. In the above equation only the terms associated with the nuclei will be considered functions of the relative inter-nuclear distance, while the electron-electron interaction will be treated as perturbation which will actually raise the Coulomb barrier between the two reacting nuclei [Lio01]. We consider the following channels:

a) The nucleus-nucleus channel

b) The atom-atom channel for Hydrogen like atoms.

In most experiments, the projectile has been considered fully stripped of its electrons which is the case at relatively high energies. However, when the projectile is in a neutral state, or at least not fully ionized, its electron cloud has to be taken into account [Eng88]. For such an interaction the total potential energy can be written:

$$V_{sc} = V_c(r) + V_{n_2e_1}(r) + V_{n_1e}(r) + V_{e_1e}(r) \tag{3.33}$$

When the two electron clouds interact, their mutual ground state wavefunction must be antisymmetric, since the electrons are identical fermions. The spatial wavefunction is necessarily symmetric, therefore antisymmetry is arranged by considering an antisymmetric spin singlet state. Since we still work with hydrogen-like atoms, the electron-electron spatial wavefunction is

$$\psi_{e_1e}(r_1, r_2) = \psi_{00}(r_1)\psi_{00}(r_2) \tag{3.34}$$

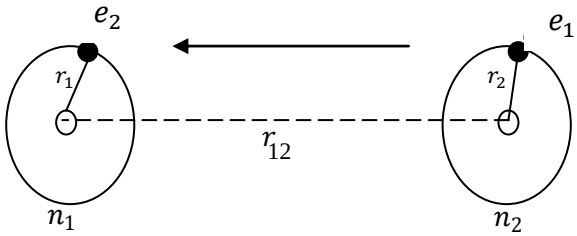

Fig 3.7. *Shematic representation of the colliding atoms*

where $\psi_{00}(r)$ is actually the usual ground state wavefunction of hydrogen-like atoms. The electrostatic potential energy of the two electrons is:

$$V_{e_1e}(r) = \int_1 \int_2 \frac{e^2}{|r_1 - r_2|} |\psi_{00}(r_1)|^2 |\psi_{00}(r_2)|^2 d^3r_1 d^3r_2 \tag{3.35}$$

where $r_{1,2}$ are the position of the two electrons [Bra83], and

$$\psi_{00}(r) = \frac{2}{\sqrt{4\pi}} \left(\frac{Z}{a_0}\right)^{3/2} \exp\left(-\frac{Zr}{a_0}\right) \tag{3.36}$$

which gives

$$V_{e_1e} = \left[\frac{1}{\pi}\left(\frac{Z}{a_0}\right)^3\right]^2 e^2 \int_0^\infty r_1^2\, dr_1\, exp\left(\frac{-2Zr_1}{a_0}\right) \int_0^\infty r_2^2 dr_2 exp\left(\frac{-2Zr_2}{a_0}\right) \int d\Omega_1 \int d\Omega_2 \frac{1}{|r_1 - r_2|} \tag{3.37}$$

In order to handle the last integral we first write $\frac{1}{|r_1 - r_2|}$ as

$$\frac{1}{|r_1 - r_2|} = \frac{1}{\left(r_1^2 + r_2^2 + 2r_1^2 r_2^2 cos\theta\right)^{1/2}} \tag{3.38}$$

where θ is the angle between $r_1\ and\ r_2$ and we choose the direction of r_1 as the Z axis for the $d\Omega_2$ integration, we then obtain:

$$\int d\Omega_2 \frac{1}{|r_1 - r_2|} = \int_0^{2\pi} d\varphi \int_{-1}^{+1} d\cos\theta \frac{1}{\left(r_1^2 + r_2^2 + 2r_1^2 r_2^2 cos\theta\right)^{\frac{1}{2}}} \tag{3.39}$$

Using the expansion

$$\frac{1}{|r_1 - r_2|} = \frac{1}{\left(r_1^2 + r_2^2 + 2r_1^2 r_2^2 cos\theta\right)^{1/2}} = \frac{1}{r_1} \sum_{l=0}^{\infty} \left(\frac{r_2}{r_1}\right)^l P_l(\cos\theta) \tag{3.40}$$

one gets

$$\int d\Omega_2 \frac{1}{|r_1 - r_2|} = \frac{2\pi}{r_1 r_2} (r_1 + r_2 - |r_1 - r_2|) \tag{3.41}$$

Besides the integration over Ω_1 gives simply

$$\int d\Omega_1 = 4\pi \tag{3.42}$$

The integration is then written as:

$$V_{e_1e} = 8e^2\left(\frac{Z}{a_0}\right)^6 \int_0^\infty r_1 dr_1 exp\left(\frac{-2Zr_1}{a_0}\right) \int_0^\infty r_2 dr_2 exp\left(\frac{-2Zr_2}{a_0}\right)(r_1 + r_2 - |r_1 - r_2|) \quad (3.43)$$

or:

$$V_{e_1e} = 8e^2\left(\frac{Z}{a_0}\right)^6 \int_0^\infty r_1 dr_1\, exp\left(\frac{-2Zr_1}{a_0}\right)\left[2\int_0^{r_1} r_2^2 dr_2 \exp\left(\frac{-2Zr_2}{a_0}\right) + 2r_1\int_{r_1}^\infty r_2 dr_2 \exp\left(\frac{-2Zr_2}{a_0}\right)\right] \quad (3.44)$$

And finally after integration over r_1 and r_2

$$V_{e_1e} = \frac{5}{8}\frac{Ze^2}{a_0} \quad (3.45)$$

That positive energy will be transferred to the relative nuclear motion, increasing the height of the Coulomb barrier.

On the other hand each of the two electrons is actually subject to the repulsive effect of a screened nucleus due to the presence of the other electron. For the combined nuclear molecule, we have $Z_t = Z_1 + Z_2$, while the usual variational procedure yields an affective atomic number for each electron [Bra83]

$$Z^{**} = Z_t - 5/16 \quad (3.46)$$

Therefore for the low energy reaction of two hydrogenlike atoms in their ground state, with equal atomic numbers Z, the interaction potential using (3.30) energy is:

$$V_{sc}(r) = \frac{Z^2e^2}{r} - 2\left[\frac{Ze^2}{r} + \frac{Ze^2}{r}\left(1 + \frac{r}{2r_0^{**}}\right)exp(-r/r_0^{**})\right] + \frac{5}{8}\frac{Z^{**}e^2}{a_0} \quad (3.47)$$

where

$$r_0^{**} = \frac{a_0}{2Z^{**}} \quad (3.48)$$

For two hydrogenlike atoms with equal charges Ze, and at astrophysical energies where screening becomes important the screened coulomb potential can be replaced by the quantity [Lio01]

$$V_{sc}(r) = \frac{Z^2e^2}{r} + U_e \tag{3.49}$$

Where

$$U_e = -2Z\left(2Z - \frac{5}{16}\right)\frac{e^2}{a_0} + \frac{5}{8}(2Z - \frac{5}{16})\frac{e^2}{a_0} \tag{3.50}$$

Which is also the screening energy for the collision of a bare nucleus Ze with a two-electron target atom [lio01].

3.5. Screening effect with excited electrons

3.5.1. The projectile in the 2s state

In the present work, we intend to extend the study of the atomic screening effect to excited states.

Let us consider the case when the projectile atom is in the excited state 2s, as the previous case the potential energy is given by

$$V_{sc} = V_c(r) + V_{n_2e_1}(r) + V_{n_1e}(r) + V_{e_1e}(r) \tag{3.51}$$

The electron-electron spatial wave function is

$$\psi_{e_1e}(r_1, r_2) = \psi_{100}(r_1)\psi_{200}(r_2) \tag{3.52}$$

With

$$\begin{cases} \psi_{100}(r) = \frac{2}{\sqrt{4\pi}}\left(\frac{Z}{a_0}\right)^{3/2}\exp\left(-\frac{Zr}{a_0}\right) \\ \psi_{200}(r) = \frac{1}{2\sqrt{2\pi}}\left(\frac{Z}{a_0}\right)^{3/2}\left(1 - \frac{Zr}{2a_0}\right)\exp\left(-\frac{Zr}{2a_0}\right) \end{cases} \tag{3.53}$$

From which the densities are given by

$$\begin{cases} |\psi_{100}(r_1)|^2 = \frac{1}{\pi}\left(\frac{Z}{a_0}\right)^3 exp\left(\frac{-2Zr_1}{a_0}\right) \\ |\psi_{200}(r_2)|^2 = \frac{1}{8\pi}\left(\frac{Z}{a_0}\right)^3\left(1 - \frac{Zr_2}{2a_0}\right)^2 exp\left(\frac{-Zr_2}{a_0}\right) \end{cases} \tag{3.54}$$

using (3.54) the potential energy becomes:

$$V_{e_1e} = \int_1 \int_2 \frac{e^2}{|r_1 - r_2|} |\psi_{100}(r_1)|^2 |\psi_{200}(r_2)|^2 d^3r_1 d^3r_2 \tag{3.55}$$

After integration one gets

$$V_{e_1e} = \frac{17}{81}\frac{Z}{a_0}e^2 \tag{3.56}$$

The screened potential using (3.29) is then:

$$V_{sc}(r) = \frac{Z^2e^2}{r} - 2\left[\frac{Ze^2}{r} + \frac{Ze^2}{r}\left(1 + \frac{3}{8}\frac{r}{r_0^{**}} + \frac{r^2}{16r_0^{**2}} + \frac{r^3}{64r_0^{**3}}\right) exp\left(\frac{-r}{2r_0^{**}}\right)\right] + \frac{17}{81}\frac{Z^{**}}{a_0}e^2 \tag{3.57}$$

Where Z^{**} is given by using the variational method [Bra83]:

$$Z^{**} = Z_t - \frac{690}{512}$$

At astrophysical energies we have

$$V_{sc}(r) = \frac{Z^2e^2}{r} + U_e \tag{3.58}$$

where:

$$U_e = -(Z_1 + Z_2)\left(Z_t - \frac{690}{512}\right)\frac{e^2}{a_0} + \frac{17}{81}\left(Z_t - \frac{690}{512}\right)\frac{e^2}{a_0} \tag{3.59}$$

3.5.2. Both atoms are in the 2s state:

In the same way we can calculate the potential energy when both atoms are in an excited state

$$V_{sc} = V_c(r) + V_{n_2e_1}(r) + V_{n_1e}(r) + V_{e_1e}(r) \tag{3.60}$$

The electron-electron spatial wave function is

$$\psi_{e_1e}(r_1, r_2) = \psi_{200}(r_1)\psi_{200}(r_2) \tag{3.61}$$

The electron-electron interaction energy is then

$$V_{e_1e} = \int_1 \int_2 \frac{e^2}{|r_1 - r_2|} |\psi_{200}(r_1)|^2 |\psi_{200}(r_2)|^2 d^3r_1 d^3r_2 \quad (3.62)$$

As the same way of the integration of the (3.35), using also (3.38), (3.39), (3.41) and (3.42), we will get:

$$V_{e_1e} = \frac{2689}{2560} \frac{Z}{a_0} e^2 \quad (3.63)$$

$$V_{sc}(r) = \frac{Z^2e^2}{r} - 2\left[\frac{Ze^2}{r} + \frac{Ze^2}{r}\left(1 + \frac{3}{8}\frac{r}{r_0^{**}} + \frac{r^2}{16r_0^{**2}} + \frac{r^3}{64r_0^{**3}}\right) exp\left(\frac{-r}{2r_0^{**}}\right)\right] + \frac{2689}{2560}\frac{Z^{**}}{a_0} e^2 \quad (3.64)$$

Where

$$Z^{**} = Z_t - \frac{690}{512} \quad (3.65)$$

At astrophysical energies we have

$$V_{sc}(r) = \frac{Z^2e^2}{r} + U_e \quad (3.66)$$

$$U_e = -(Z_1 + Z_2)\left(Z_t - \frac{690}{512}\right)\frac{e^2}{a_0} + \frac{2689}{2560}\left(Z_t - \frac{690}{512}\right)\frac{e^2}{a_0} \quad (3.67)$$

3.6. Astrophysical factor S(E) of $^3He(^3He, 2p)^4He$ at solar energy

3.6.1.Mechanism of interaction:

In main sequence stars of low mass, such as the sun, energy is produced predominantly by the hydrogen burning pp chain. The $^3\mathrm{He}(^3\mathrm{He}, 2\mathrm{p})^4\mathrm{He}$ reaction is one of the reactions involved in this chain. It can be visualized as a direct process in the entrance channel leading to three possible decay-modes in the exit channel: (i) a direct breakup into 3 particles of the exit channel ($2p+^4He$); (ii) a sequential breakup into $p+^5Li$ with the subsequent decay $^5Li \rightarrow p+^4He$; and (iii) a sequential breakup $2p+^4He$ with the subsequent decay $2p \rightarrow p + p$. The early studies were carried out over a wide range of beam energies and to as low as $E_{cm} \simeq 90\ kev$. From the observed particle spectra it followed that the sequential processes prevail at the higher energies ($E_{cm} \geq 1Mev$) but the direct breakup is dominant at lower energies.

The observed energy dependence of the astrophysical $S(E)$ factor [Kra87b],

$$S(E) = \sigma(E)Exp(2\pi\eta) \tag{3.68}$$

where $2\pi\eta = 4.86/E^{1/2}$ (with the c.m energy Ein Mev), has been fitted to the polynomial function

$$S(E) = S(0) + S'(0)E + \frac{1}{2}S''(0)E^2 \tag{3.69}$$

May & Clayton suggested a mechanism for This^{3}He(^{3}He, 2p)^{4}He interaction at low beam energy, in which a neutron tunnels from one^3He to the other, unimpeded by the coulomb barrier, up to a radial distance where the nuclei overlap appreciably. In this model, a diproton remains and subsequently fissions into 2 protons. The calculated $S(E)$ factor described the observed energy dependence of the data very well, thus providing confidence in the extrapolation via the above polynomial function.

The magnitude of the $S(E)$ factor is of special interest in relation to the solar neutrino problem. Based partially on theoretical arguments, it has been suggested that at low energy resonance might exist in this reaction. If it is sufficiently low and narrow in reaction energy, it might have been unobserved in previous direct measurements. Such a low energy resonance would significantly enhance the$^3He+^3He$ route in the pp chain (86%) at the expense of the alternative$^3He+^4He$ branch (chain II and III, 14%). If so, the discrepancy between predicted and observed solar-neutrino fluxes might be accounted for or at least decreased. This expected resonance would correspond to an excited state in^6Be near the$^3He+^3He$ thershold ($E_x \simeq 11.6Mev$). however, the search for this state, using a variety of other nuclear reactions, has not been successful: none of these reactions that populate^6Be showed any excited state near the$^3He+^3He$ thershold.

In 1974 Dwarakanath carried out a search for this hypothetical resonance state in a more direct way by extending The^{3}He(^{3}He, 2p)^{4}He reaction studies down to $E_{cm} = 30\ kev$. Although the data might suggested an increase in the $S(E)$ factor at the lowest energies, the large uncertainties in the data points (about 200%) precluded any confirmation of the existence of this resonance at least down to $E_{cm} = 40\ kev$. Below 40 keV the available data neither confirmed nor ruled out its existence.

In the absence of such a resonance the calculated solar neutrino flux for the^{37}Cl experiment depends on the $S(0)$factor of The^{3}He(^{3}He, 2p)^{4}He reaction.

3.6.2. Calculation of the screened astrophysical factor:

The aim of this section is to study the effect of the screening by excited states electrons of the colliding atoms for the determination of the astrophysical S factor we use experimental data(NACRE), the appropriate treatment of a low energy experiment should take into account screening effects in order to calculate the respective values of $S(E)$.

The S factor data have been approximated by a polynomial of degree 2, the polynomial coefficients have been obtained where the experimental data have been weighted by their absolute error($E\ in\ MeV, S\ in\ MeV.b$): $S(E) = 5.5 - 3.1E + 1.4\,E^2$. Due to the screening effect at low energy the S factor must be written as

$$S_{SC}(E) = (5.5 - 3.1E + 1.4E^2)\exp\left(\pi\eta\frac{U_e}{E}\right) \tag{3.70}$$

where U_e is determined in the previous section equation (3.67).
In Theodore's calculation[Lio00]: $U_e = -338\ eV$; in our's

$$U_e = -(Z_1 + Z_2)\left((Z_1 + Z_2) - \frac{690}{512}\right)\frac{e^2}{a_0} + \frac{2689}{2560}\left((Z_1 + Z_2) - \frac{690}{512}\right)\frac{e^2}{a_0} \tag{3.71}$$

For The^{3}He(^{3}He, 2p)^{4}He reaction we have $Z_1 = Z_2 = 2$ and the corresponding screening energy obtained through the above model Is

$$U_e = -439eV \tag{3.72}$$

Two approximations of the unscreened *S(E)* have been used: linear and quadratic

3.6.2.1. The linear approximation:

In this approximation only the constant and linear term in E are used. Fig (3.8) and (3.9) give respectively our result, the Liolios result and a comparison between them.

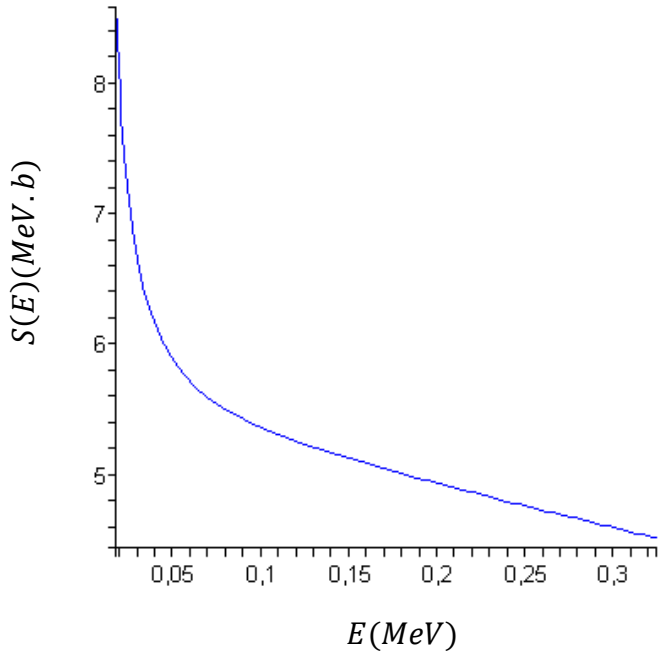

Fig3.8 *S Factor representation in the BES model*

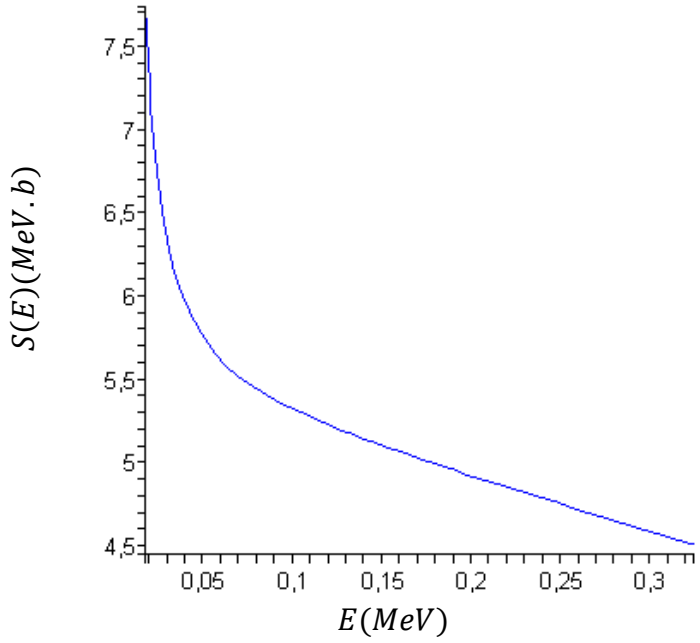

Fig3.9 *S Factor representation in the Liolios's model*

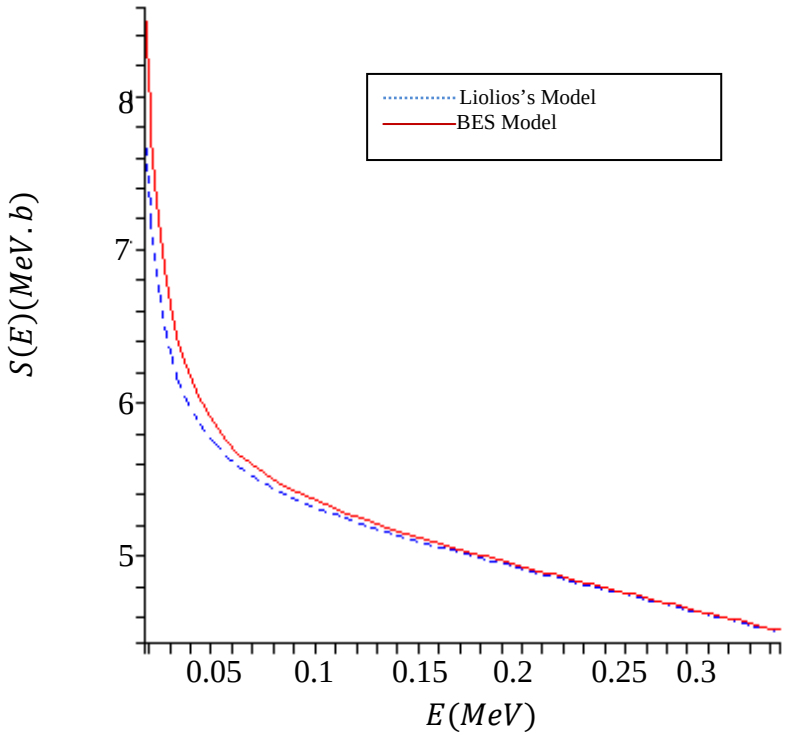

Fig3.10 *Comparison between the two model in the linear approximation.*

3.6.2.2. The quadratic approximartion

A better result from Liolios model can be obtained if the quadratic term is included in $S(E)$. Fig (3.11) gives our result and a comparison with Liolios model is given in fig (3.13).

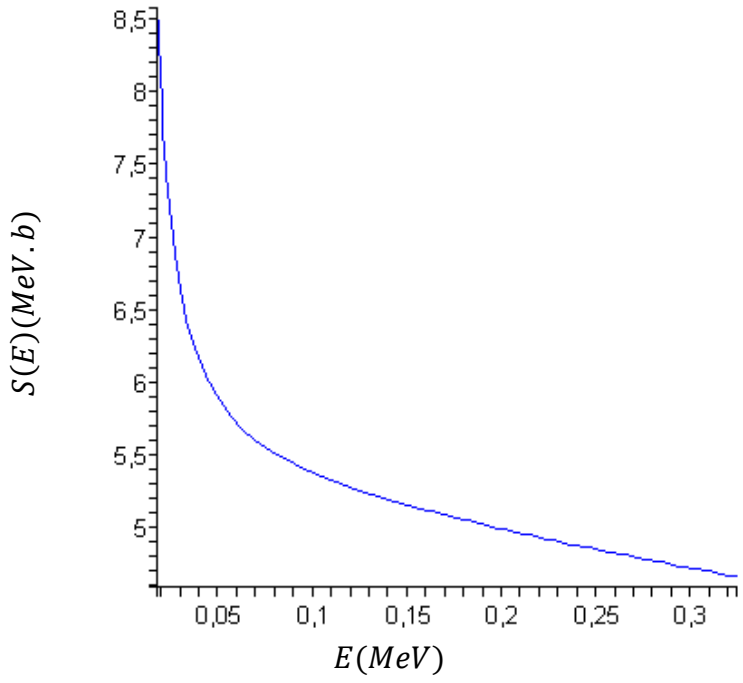

Fig3.11 *S Factor representation in the BES model for the quadratic order approximation*

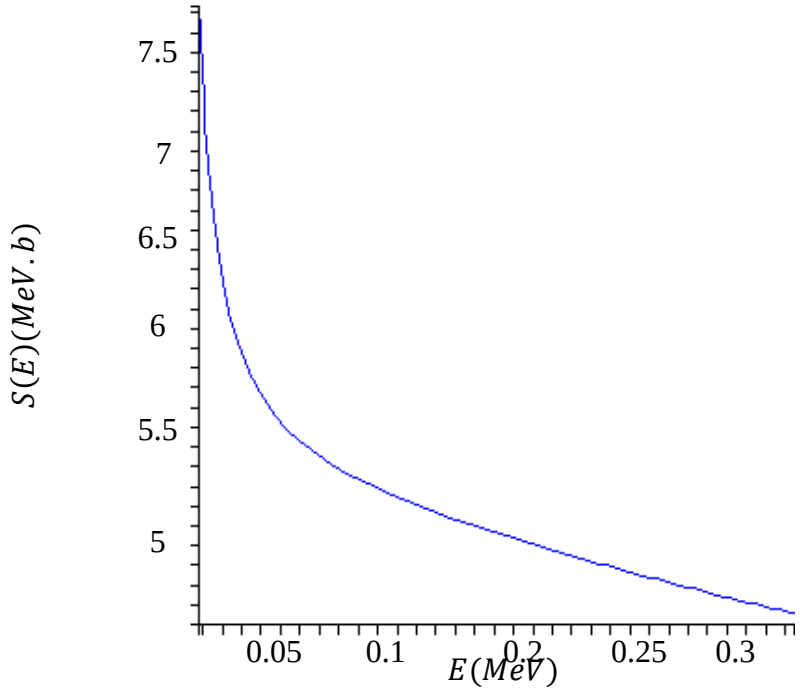

Fig3.12 *S Factor representation in the Liolios's model for the quadratic order approximation*

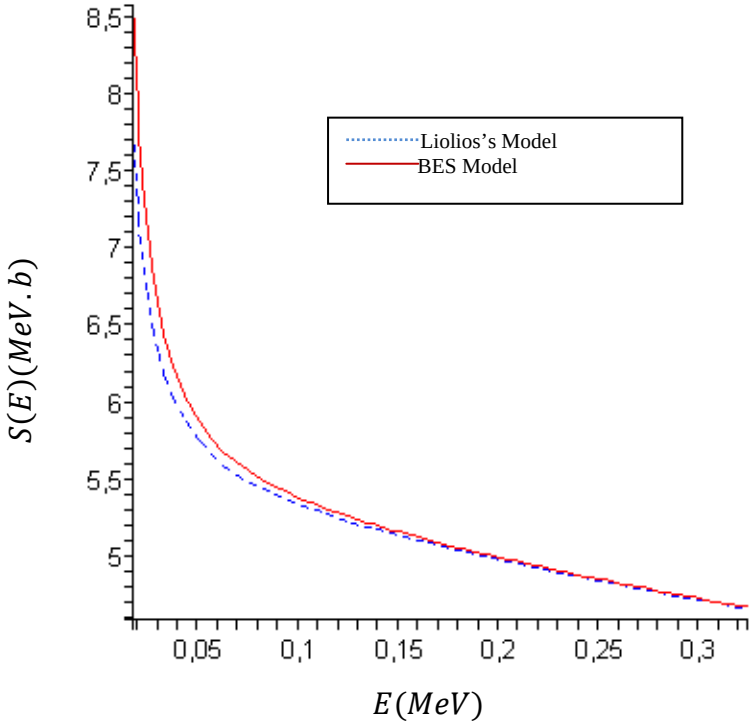

Fig3.13 *Comparison between the two models*

Our work show that the occurrence of excited states in the colliding atoms increase the screening effect in low energy fusion reactions.

Chapter 4

MAGNETICALLY ENHANCED SCREENING IN FUSION REACTIONS

4.1. Strong magnetic field in astronomy:

Magnetic white dwarfs have surface fields of $10^{3-4}T$ [Cha92]. For example, the spectrum of the hot white dwarfs Fige[L795-5] shows well resolved narrow Zeeman lines corresponding to a magnetic field of 1.800 T. The narrowness of these lines indicates a fairly uniform field strength over the entire surface. In GD90, which has a hydrogen atmosphere, the H_β line appears as a classic triplet at 479.3, 485.7, and 491.8 nm corresponding to 500 T field. The H_γ is seen as broad absorption centered at 433 nm, the triplet obscured by the quadratic Zeeman effects many components. Another star, BPM25114, is seen in the southern skies and its spectrum fitted to model atmosphere calculations and a magnetic fields of $3.6 \times 10^3 T$.

The origin of such fields on white dwarfs may lie in flux conservation in the core during the collapse of a star, the high conductivity of a carbon-burning core preserving the value RB^2. These simple scalings when a star collapses suggest fields up to $10^5 T$ for white dwarfs and $10^9 T$ for collapse to the smaller radius of neutron star. An alternative is that they have originated from Ap stars known to have fields of 0.03-3 T with similar flux conservation during their collapse. Magnetic stars are modeled as oblique rotators, with the dipolar magnetic field inclined to the rotation axis[Rau03].

Rotating magnetic white dwarfs which are accreting matter from a companion have proved particularly interesting. DQHer has a eclipsing binary system with orbital period 4.6 hours. Matter being accreted onto white dwarfs is speeding up the rotation and a field of 100T has been deduced; strong enough to channel the accretion flow onto the poles. Direct spectral evidence has not been seen from these objects, possibly swamped by emission from the surrounding accretion disk, but in AMHer, polarized cyclotron and X ray emission from such accreted material has been seen the very strong polarization, both circular and linear, argues for field strength above $10^3 T$, the channeling of the accretion flow by such a field accounting for the X-ray emission at 5nm, GRW+70°247 is the brightest and one of the most strongly polarized of the magnetic white dwarfs, peaks in the circular polarization at 1.3 and 0.45μm

attributed to first and third cyclotron harmonics of a field in excess of 10^4T. The strongest field known is about 10^5T on PG1031+234, deduced from its spectrum and polarization.

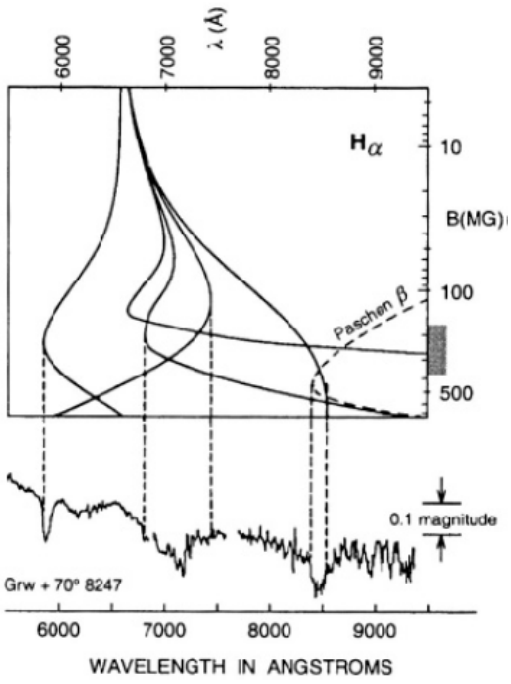

Fig 4.1: Stationary H_α Balmer transitions of Hydrogen compared with the optical spectrum of GRw+70°8247,taken from [Cha92]

Fields of 10^4T which are far from being perturbative pose the problems but elaborate perturbative elaborate numerical calculations now provide reliable energies for low lying states. Interestingly, the $Ly_\alpha 1s, m = 0 - p, m = -1$ transitoin wave length as a function of field strength reaches a stationary value around 5×10^4T, the zero field value if 121.6 nm reaching a maximum of 134.3 nm before decreasing again. This stationarity, so that the wavelength is relatively insensitive to variations in B about that value made possible the identification of a line at 134.7 nm observed by the International Ultraviolet Explorer [I.U.E] satellite from GRW+70°247. This was happy coincidence because variations in B across the surface tend other wise to smear out the transition. Other stationary transitions have since been used to identify the magnetic fields of various white dwarfs, an example is shown in Fig4.1.

Neutron stars have even stronger magnetic fields, of the order of 10^8T in ratio pulsars and somewhat smaller $10^{5-7}T$ in binary pulsars. X-ray binaries and also certain neutron stars are deeded into low and high mass types, depending on the mass of non-degenrate companion

star. Most high mass binaries have magnetic fields larger than 10^4 and accrete from an O or B type star. Their ages are less than $10^7 T$ years whereas low mass binaries are much older $> 10^9 years$. Their fields range up to $10^6 T$ Gamma ray burst sources show lines in the 20 to 70 KeV range; again indicators of cyclotron emission between Landau level in fields of $10^8 T$. These objects are presumed to be neutron stars with rotation periods larger then a few seconds.

4.2.Motion of particle in a uniform magnetic field:

4.2.1.Solution in the Cartesian coordinates:

Let us determine the energy level of a particle with spin *s* and magnetic moment μ moving in constant uniform magnetic field [Lan67], the vector potential of the uniform field is taken in the form

$$A_x = -H_y; A_y = A_Z = 0 \tag{4.1}$$

(*the z axis being taken in the direction of the field)*

The Hamiltonian then becomes

$$H = \frac{1}{2m}(p_x - \frac{e}{c}H_y)^2 + \frac{p^2{}_y}{2m} + \frac{p_z^2}{2m} - (\frac{\mu}{s})S_z H \tag{4.2}$$

First of all, we notice that the operator S_z commutes with the Hamiltonian, since the latter does not contain the operators of the other components of the spin. This means that the z-component of the spin is conserved, and therefore that S_z can be replaced by the eignenvalue $S_z = \sigma$. Then the spin dependence of the wave function becomes unimportant, and ψ in Schrödinger's equation can be taken as the ordinary coordinate function. For this function we have the equation

$$\frac{1}{2m}\left[\left(p_x - \frac{eH_y}{c}\right)^2 + p_y^2 + p_z^2\right]\psi - \frac{\mu}{s}\sigma H\psi = E\psi \tag{4.3}$$

The Hamiltonian of this equation does not contain the coordinates *x* and *z* explicitly. The operators p_x ; p_z therefore also commute with the Hamiltonian, i.e. the *x* and *z* components of the generalized momentum are conserved. We accordingly seek ψ in the form

$$\psi = e^{\frac{i}{\hbar}(p_x x + p_z z)}\chi(y) \tag{4.4}$$

The eigenvalues $p_x \; and \; p_z$ take all values. Since $A_Z = 0$, the z-component of the generalized momentum is equal to the ordinary momentum component mv_z. Thus the velocity of the particle in the direction of the field can take any value; we can say that the motion along the field is " not quantized".

Substituting (4.4) in (4.3) we obtain the following equation for the function $\chi(y)$:

$$\chi'' + \frac{2m}{\hbar}\left[\left(E + \frac{\mu\sigma}{s}H - \frac{p_z^2}{2m}\right) - \frac{1}{2}m{\omega_H}^2(y - y_0)^2\right]\chi = 0 \tag{4.5}$$

With the notation $y_0 = -\frac{cp_x}{eH}$ and

$$\omega_H = |e|H/mc \tag{4.6}$$

Equation (4.5) is formally identical to Schrödinger's equation for a linear oscillator, oscillating with frequency ω_H. Hence we can conclude immediately that the expression $\left(E + \frac{\mu\sigma}{s}H - \frac{p_z^2}{2m}\right)$ which takes the part of the oscillator energy, can have the values $\left(n + \frac{1}{2}\right)\hbar\omega_H, where \; n = 0; 1; 2; \ldots$

Thus we obtain the following expression for the energy levels of a particle in a uniform magnetic field

$$E = \left(n + \frac{1}{2}\right)\hbar\omega_H + \frac{p_z^2}{2m} - \frac{\mu\sigma}{s} \tag{4.7}$$

The first term here gives the discrete energy values corresponding to motion in a plane perpendicular to the field; they are called *Landau levels*. For an electron, $\frac{\mu}{\sigma} = -\frac{\hbar}{mc}|e|$, and formula (4.7) becomes

$$E = \left(n + \frac{1}{2} + \sigma\right)\hbar\omega_H + \frac{p_z^2}{2m} \tag{4.8}$$

The eigenfunctions $\chi_n(y)$ corresponding to the energy levels are:

$$\chi_n(y) = \frac{1}{\pi^{\frac{1}{4}}{a_H}^{\frac{1}{2}}\sqrt{2^n n!}}\, exp\left[-\frac{(y-y_0)^2}{2a_H^2}\right] H_n\left(\frac{y-y_0}{a_H}\right) \tag{4.9}$$

where $a_H = \sqrt{\frac{\hbar}{m\omega_H}}$

In classical mechanics, the motion of particles in a plane perpendicular to the field H (x-y plane) takes place in a circle about a fixed centre.

4.2.2.Solution in the cylindrical coordinates:

We will find the wave function of an electron in a uniform magnetic field in states in which it has definite values of the momentum and angular momentum in the direction of the field.

In cylindrical polar coordinates ρ, ϕ, z with the z-axis in the direction of the field, the vector potential has components $A_\phi = \frac{1}{2} H\rho; A_z = A_\rho = 0$, and Schrödinger's equation is:

$$-\frac{\hbar^2}{2M}\left[\frac{1}{\rho}\frac{\partial}{\partial\rho}\left(\rho\frac{\partial\psi}{\partial\rho}\right)+\frac{\partial^2\psi}{\partial z^2}+\frac{1}{\rho^2}\frac{\partial^2\psi}{\partial\phi^2}\right]-\frac{1}{2}i\hbar\omega_H\frac{\partial\psi}{\partial\phi}+\frac{1}{8}M\omega_H^2\rho^2\psi=E\psi \qquad (4.10)$$

We seek a solution in the form

$$\psi=\frac{1}{\sqrt{2\pi}}R(\rho)e^{im\phi}e^{p_z z/\hbar} \qquad (4.11)$$

The radial function $R(\rho)$ satisfy the radial equation

$$\frac{\hbar^2}{2M}\left(R''+\frac{R'}{\rho}-\frac{m^2R}{\rho^2}\right)+\left[E-\frac{p_z^2}{2M}-\frac{1}{8}M\omega_H^2\rho^2-\frac{1}{2}i\hbar\omega_H m\right]R=0 \qquad (4.12)$$

Defining a new independent variable $\xi=(M\omega_H/2\hbar)\rho^2$, we can write this equation in the form

$$\xi R''+R'+\left(-\frac{1}{2}\xi+\beta-\frac{m^2}{4\xi}\right)R=0 \qquad (4.13)$$

where

$$\beta=\frac{1}{\hbar\omega_H}\left(E-\frac{p_z^2}{2M}\right)-\frac{1}{2}m \qquad (4.14)$$

As $\xi\to\infty$ the required function behaves as $e^{-\frac{1}{2}\xi}$, and for $\xi\to 0$ as $\xi^{|m|/2}$. Accordingly we seek a solution in the form

$$R(\xi)=e^{-\frac{\xi}{2}}\xi^{\frac{|m|}{2}}w(\xi) \qquad (4.15)$$

The equation for $w(\xi)$ is satisfied by the confluent hyper-geometric function

$$w = F\left\{-\left(\beta - \frac{1}{2}|m| - \frac{1}{2}\right), |m| + 1, \xi\right\} \quad (4.16)$$

If the wave function is everywhere finite, the quantity $\left(\beta - \frac{1}{2}|m| - \frac{1}{2}\right)$ must be non-negative integer n_ρ. The energy levels are then given by the formula

$$E = \hbar\omega_H\left(n_\rho + \frac{1}{2}|m| + \frac{1}{2}m + \frac{1}{2}\right) + \frac{p_z^2}{2M} \quad (4.17)$$

The corresponding radial wave functions are

$$R_{n\rho m}(\rho) = \frac{1}{a_H^{1-|m|}|m|!}\left[\frac{(|m|+n_\rho)!}{2^{|m|}n_\rho!}\right]^{1/2} \exp\left(-\frac{\rho^2}{4a_H^2}\right)\rho^{|m|} \times F\{n_\rho|m| + 1, \rho^2 2a_H^2\} \quad (4.18)$$

Where $a_H = \sqrt{\hbar/M\omega_H}$. These functions are normalized by the condition

$$\int_0^\infty R^2\rho d\rho = 1 \quad (4.19)$$

The hyper-geometric function is here a generalized Laguerre polynomial.

4.3.Binding energy of hydrogen atoms in a strong magnetic field:

4.3.1.Introduction:

When studying matter in magnetic fields, the natural (atomic) unit for the field strength, B_0, is set by equating the electron cyclotron energy $\hbar\omega_{ce}$ to the characteristic atomic energy $\frac{e^2}{a_0} = 13.6\ eV$, where a_0 is the Bohr radius, or equivalently by $R = a_0$. [Lai06]

Thus it is convenient to define a dimensionless magnetic field *b* via:

$$b = \frac{B}{B_0};\ B_0 = \frac{m_e^2 e^3 c}{\hbar^3} = {\alpha_0}^2 B_Q = 2.3505 \times 10^9 Gauss$$

Where $\alpha_0 = \frac{1}{137}$ is the fine structure constant.

For $b \gg 1$, the cyclotron energy $\hbar\omega_{ce}$ is much larger than the typical Coulomb energy, so that the properties of atoms, molecules and condensed matter are qualitatively changed by the magnetic field. Instead, the Coulomb forces, and the electron in an atom settle into the ground Landau level. Because of the extreme confinement of the electrons in the transverse

direction, the Coulomb force becomes much more effective in binding the electrons along the magnetic field direction. The atom attains a cylindrical structure.

Note that when studying bound states (atoms, molecules, and condensed matter) in strong magnetic fields, it is adequate to use nonrelativistic quantum mechanics, even for $B \gg B_Q$. The nonrelativistic treatment of bound states is valid for two reasons:

(i): For electrons in the ground Landau level, so the equation

$$E_n = [c^2p^2 + m_e^2c^4\left(1 + 2n\frac{B}{B_Q}\right)]^{0.5} \tag{4.20}$$

for the free electron energy reduces to $E \approx m_e^2c^2 + \frac{p^2}{2m_e}$ for $pc \ll m_ec^2$, the electron remains non relativistic in the z direction (along the field axis) as long as the binding energy E_B is much less than m_ec^2

(ii) The shape of the Landau wave function in the relativistic theory is the same as in the non-relativistic theory.

4.3.2.Hydrogen atom in a strong magnetic field:

In strong magnetic field with $b \gg 1$, the electron is confined to the ground Landau level ("adiabatic approximation"), and the Coulomb potential can be treated as a perturbation. Assuming infinite proton mass, the energy spectrum of the H atom is specified by two quantum numbers (m, v) where m measures the mean transverse separation between the electron and the proton, while v specifies the number of nodes in the z-wavefunction.

In large magnetic fields a hydrogen atom is compressed both perpendicular and parallel to the field direction. In a sufficiently strong magnetic field ($B \geq 10^{12}$G), the Schrödinger equation for the dynamics of the electron separates into axial and perpendicular (azimutal and radial) equation. As the potential is axisymmetric around the direction of the magnetic field, we expect no azimutal dependence in the ground state wave function of the electron.

In the direction perpendicular to the magnetic field, the wave function can be obtained [See §a]. This azimutal wave function is denoted by two quantum numbers n and m. Here we take $n = 0$, as the $n > 0$ solutions are less bound and therefore provide less shielding [Hey96].

The perpendicular wave function has the same form as the Landau wave function for an electron in a magnetic field:

$$R_{0m}(\rho,\theta) = \frac{1}{\sqrt{2^{m+1}\pi m!}a_H^{m+1}}\rho^m \exp\left(-\frac{\rho^2}{4a_H^2}\right)e^{im\theta} \quad (4.21)$$

where $a_H = \sqrt{\frac{\hbar}{m_e\omega_H}} = \sqrt{\frac{\hbar c}{|e|H}}$

a. axial wave function:

In a sufficiently strong magnetic field a_H is very small compared to the Bohr radius a_0.

Along the direction of the magnetic field, the electron experiences an effective potential

$$V_{eff,0m}(z) = \langle R|V(r)|R\rangle = \int_0^\infty -\frac{e^2}{\sqrt{z^2+\rho^2}}R_{0m}^2(\rho)2\pi\rho d\rho \quad (4.22)$$

where

$$R_{0m}^2(\rho) = \frac{(-1)^m}{2\pi m!}\frac{1}{a_H^2}\left(\frac{d}{d\beta}\right)^m\left[\exp\left(-\beta\frac{\rho^2}{2a_H^2}\right)\right]\Big|_{\beta=1} \quad (4.23)$$

So

$$V_{eff,0m}(z) = \int_0^\infty -\frac{e^2}{\sqrt{z^2+\rho^2}}\frac{(-1)^m}{2\pi m!}\frac{1}{a_H^2}\left(\frac{d}{d\beta}\right)^m\left[\exp\left(-\beta\frac{\rho^2}{2a_H^2}\right)\right]\Big|_{\beta=1}2\pi\rho d\rho \quad (4.24)$$

$$= -\frac{e^2}{a_H}\sqrt{\frac{\pi}{2}}\frac{(-1)^m}{m!}\left(\frac{d}{d\beta}\right)^m\left[\frac{1}{\sqrt{\beta}}(\beta z^2/2a_H^2)\mathrm{erfc}\left(\sqrt{\beta}|z|/\sqrt{2}a_H\right)\right]\Big|_{\beta=1} \quad (4.25)$$

which for large z approaches $-e^2/z$.

The Schrödinger equation is solved using the variational methods. Let $Z(z)$ be the trial function, then one has to minimize the integral

$$I = \langle Z|H|Z\rangle = \int_{-\infty}^{+\infty}\left[\frac{\hbar^2}{2m_e}(\nabla_z Z)^2 + V_{eff}Z^2\right]dz \quad (4.26)$$

Prior to our work J.S.Heyl and L.Hernquist [Hey96] used a Gaussian trial function depending on a parameter a_z :

$$Z(z) = \frac{1}{\sqrt[4]{2\pi}} \frac{1}{\sqrt{a_z}} exp\left(\frac{-z^2}{4a_z^2}\right) \tag{4.27}$$

In the present work; we have chosen a trial function with the same z dependence as the case of zero magnetic field:

$$Z(z) = \frac{1}{\sqrt{a_z}} exp\left(\frac{-|z|}{a_z}\right) \tag{4.28}$$

Because our function is even, the integral becomes:

$$I = 2\left[\int_0^\infty \frac{\hbar^2}{2m} \frac{1}{a_z^3} exp\left(\frac{-2|z|}{a_z}\right) dz - \frac{e^2}{a_H}\sqrt{\frac{\pi}{2}} \int_0^\infty exp\left(\frac{z^2}{2a_H^2} - \frac{2|z|}{a_z}\right) erfc\left[\frac{z}{\sqrt{2}}\right] \frac{1}{a_z} dz\right] \tag{4.29}$$

Instead of z one introduces a new variable u through $u = \frac{z}{a_H}$. Besides it is convenient to define the dimensionless parameter $\alpha = \frac{a_z}{a_H}$. This gives

$$I = 2\left[\int_0^\infty \frac{\hbar^2}{2m} \frac{{a_H}^4}{a_z^3} \frac{1}{a_H^3} exp\left(\frac{-2u}{\alpha}\right) du - \frac{e^2}{a_H}\sqrt{\frac{\pi}{2}} \int_0^\infty exp\left(\frac{u^2}{2} - \frac{2u}{\alpha}\right) erfc\left[\frac{u}{\sqrt{2}}\right] \frac{1}{\alpha} du\right] \tag{4.30}$$

The first integral can be easily computed to get

$$I = E_H \frac{a_0}{a_H}\left[\frac{1}{\alpha^2}\frac{a_0}{a_H} - \frac{4}{\alpha}\sqrt{\frac{\pi}{2}} \int_0^\infty exp\left(\frac{u^2}{2} - \frac{2u}{\alpha}\right) erfc\left[\frac{u}{\sqrt{2}}\right] du\right] \tag{4.31}$$

Table.1 lists the results for the minimization for several magnetic field strength, and compared with the eigenvalues for the energy of the bound state obtained by Ruder et al [Rud83] and Hey and Hernquist [Hey96].

Because of our choice of the trial wave function, our energies are roughly similar to those found by Heyl et al.

Note that, the field strength at which magnetic field binding begins to dominate the Coulomb force is established by equating $\sqrt{\frac{2\hbar}{m\omega}} = a_0$, this transition to the intense magnetic field [IMF] regime occurs at $B = 4.7 \times 10^9 G$ [Kel72]

Ruder et al [Rud83]		*Heyl et al[Hey96]*		*Our results*	
B(G)	$E_{m=0}(Ry)$	$\alpha_{m=0}$	$E_{m=0}(Ry)$	$\alpha_{m=0}$	$E_{m=0}(Ry)$
4.7×10^{9}	2.04	1.14	1.77	2.34	1.70026
4.7×10^{10}	4.43	2.00	4.18	4.18	4.043
4.7×10^{11}	9.45	3.79	8.91	7.92	8.83
4.7×10^{12}	18.6	7.77	17.1	16.02	17.59
4.7×10^{13}	-	17.3	29.6	34.66	31.93
4.7×10^{14}	-	38.1	47.0	79.63	53.17
4.7×10^{15}	-	102.	69.6	190.12	81.02
4.7×10^{16}	-	265.	97.7	477.04	108.89

Table 1 *: Results of the minimization giving the optimal* $\alpha_{m=0}$ *and the corresponding ground state energy for different values of the magnetic field.*

4.4.Screening potential:

4.4.1.Introduction:

In the presence of a strong magnetic field ($B \gtrsim 10^{12} G$), the reaction rates are many orders of magnitude higher than in the unmagnetized case. This problem has already been treated by Heyl [Hey 96]. In this work we will propose a new solution using the results obtained in section (4.3.2).

4.4.2. Heyl's Potential

When solving problems one often looks for electrostatic analogs. In this way, Heyl et al [Hey96] have looked for a gravitational analog to an electrostatic problem. The density of the electron is constant and concentric, similar homoemoids. For this density distribution the potential is directly solvable[Bin87].

$$\Phi(\vec{x}) = -\pi G\left(\frac{a_2 a_3}{a_1}\right)\int_0^{\infty}\frac{\psi(\infty)-\psi(m)}{\sqrt{(\tau+a_1^2)(\tau+a_2^2)(\tau+a_3^2)}}d\tau \tag{4.32}$$

where:

$$m^2 = a_1^2\sum_{i=1}^{3}\frac{x_i^2}{a_i^2+\tau} \tag{4.33}$$

and

$$\psi(m) = \int_0^{m^2}\rho(m^2)d\,m^2 \tag{4.34}$$

In the work of Heyl et al [Hey96], $G = -e^2, a_1 = a_2 = a_H, a_3 = a_z$, so the last expression becomes:

$$\psi(m) = \frac{1}{a_z\pi\sqrt{2\pi}}\left[1-\exp\left(-\frac{m^2}{2a_H^2}\right)\right] \tag{4.35}$$

Substituting these results into equation (4.34), and let $\bar{r} = \frac{r}{a_H}, \bar{z} = \frac{z}{a_H} and\ u = \frac{\tau}{a_H^2}$, this gives the new equation:

$$\Phi(\vec{x}) = \frac{e^2}{a_H}\frac{1}{\sqrt{2\pi}}\int_0^{\infty}\frac{exp\left\{-\frac{1}{2}\left[\frac{\overline{r^2}}{1+u}+\frac{\overline{z^2}}{\alpha^2+u}\right]\right\}}{(1+u)\sqrt{\alpha^2+u}}du \tag{4.36}$$

Using the previous definition of α, the potential at the center of the electron cloud $(r = 0, z = 0)$ is given by

$$\Phi(0,0) = \frac{e^2}{a_H}\frac{2}{\sqrt{2\pi}}\frac{ln\left(\alpha+\sqrt{\alpha^2-1}\right)}{\sqrt{\alpha^2-1}} \tag{4.37}$$

We can expand this potential in a series:

$$\Phi(0,0) = \frac{e^2}{a_H}\frac{2}{\sqrt{2\pi}}\left[\frac{4}{3}-\frac{1}{3}\alpha+\frac{2}{15}(\alpha-1)^2-\frac{2}{35}(\alpha-1)^3+\cdots\right] \tag{4.38}$$

4.4.3. BES potential

In the present work, the density is:

$$\rho(r,z) = \frac{1}{a_H^2}\frac{1}{a_z}\frac{1}{2\pi} exp\left[-\left(\frac{r^2}{2a_H^2}+\frac{2|z|}{a_z}\right)\right] \quad (4.39)$$

$$= \frac{1}{k} exp(-Ar^2) exp\left(-\frac{|z|}{\Lambda}\right) \quad (4.40)$$

where $k = 2\pi a_H^2 a_z$, $A = \frac{1}{2a_H^2}$, $\frac{1}{\Lambda} = \frac{2}{a_z}$

We will search the electrostatic potential by solving the equation of Poisson for the above density, in atomic units

$$\Delta\Phi = -\rho \quad (4.41)$$

$\rho(r,z)$ is separable into a product of a function of r by a function of z. A possible solution of equation (4.41) is then given by:

$$\Phi(r,z) = R(r)Z(z) \quad (4.42)$$

Using this form, equation (4.41) becomes

$$\frac{\partial^2\Phi}{\partial z^2} + \frac{1}{r}\frac{\partial}{\partial r}\left(r\frac{\partial\Phi}{\partial r}\right) = -\rho \quad (4.43)$$

and more explicitly

$$R(r)\frac{\partial^2 Z}{\partial z^2} + Z(z)\frac{1}{r}\frac{\partial}{\partial r}\left(r\frac{\partial R}{\partial r}\right) = -\rho \quad (4.44)$$

We divide by $Z(z).R(r)$, to get

$$\frac{1}{Z(z)}\frac{\partial^2 Z}{\partial z^2} + \frac{1}{R(r)}\frac{1}{r}\frac{\partial}{\partial r}\left(r\frac{\partial R}{\partial r}\right) = -\frac{1}{k}\frac{exp(-Ar^2)}{R(r)}\frac{exp(-\Lambda^{-1}|z|)}{Z(z)} \quad (4.45)$$

If we choose $Z(z) = exp\left(-\frac{|z|}{\Lambda}\right)$, we will obtain

$$\frac{1}{Z(z)}\frac{\partial^2 Z}{\partial z^2} = -\frac{1}{R(r)}\frac{1}{r}\frac{\partial}{\partial r}\left(r\frac{\partial R}{\partial r}\right) - \frac{1}{k}\frac{exp(-Ar^2)}{R(r)} \quad (4.46)$$

This is an equality between two functions each of them depends on a single independent variable. This is possible only if each member is constant.

$$\begin{cases} \frac{1}{Z(z)}\frac{\partial^2 Z}{\partial z^2} = C & (4.47.1) \\ \frac{1}{R(r)}\frac{1}{r}\frac{\partial}{\partial r}\left(r\frac{\partial R}{\partial r}\right) + \frac{1}{k}\frac{exp(-Ar^2)}{R(r)} = -C & (4.47.2) \end{cases}$$

From (4.47.1) and our choice of $Z(z)$ we obtain the value of the constant $C = \Lambda^{-2}$. The differential equation for $R(r)$ is then:

$$\frac{1}{r}\frac{\partial}{\partial r}\left(r\frac{\partial R}{\partial r}\right) + \Lambda^{-2}R(r) = -\frac{1}{k}exp(-Ar^2) \quad (4.48)$$

The solution of this differential equation is

$$R(r) = C_1 Y_0(\Lambda^{-1}r) + C_2 J_0(\Lambda^{-1}r) + \frac{1}{2k}\pi \int r Y_0(\Lambda^{-1}r) exp(-Ar^2)\, dr \times J_0(\Lambda^{-1}r) - \frac{1}{2k}\pi \int r J_0(\Lambda^{-1}r) exp(-Ar^2)\, dr \times Y_0(\Lambda^{-1}r) \quad (4.49)$$

This solution can not easily be handled; since we are interested only by the solution near zero, we will reduce the right member of this equation to the first term in the Taylor expansion:

$$exp(-Ar^2) = 1 - Ar^2 + A^2r^4 + \cdots \quad (4.50)$$

We substitute the development of the exponential in the equation (4.48), and the solution is then

(i) *Zero order solution*: if one keeps only the first term in the expansion, the solution would be

$$R(r) = C_2 J_0(\Lambda^{-1}r) - \frac{\Lambda^2}{k} \quad (4.51)$$

where $J_0(\Lambda^{-1}x)$ are the Bessel functions. Note that $\lim_{r\to 0} Y_0(\Lambda^{-1}r) = -\infty$ so $C_1 = 0$

Using (4.42) the associate potential is then:

$$\Phi(r,z) = \left[C_2 J_0(\Lambda^{-1}r) - \frac{\Lambda^2}{k}\right] exp(-\Lambda^{-1}|z|) \quad (4.52)$$

From the previous definition of Λ^{-1} and k, the potential at the center of the electron cloud $(r = 0, z = 0)$ is given by:

$$\Phi(0,0) = -e^2 \left[C_2 J_0(\Lambda^{-1}r) - \frac{\alpha}{8\pi a_H}\right] \quad (4.53)$$

(ii) *First order solution*: a more realistic solution is obtained if the second term in the expansion is included. It describes the decrease of the charge density. So the solution becomes now:

$$R(r) = C_2 J_0(\Lambda^{-1}r) + \frac{-\Lambda^{-2} - 4A + A\Lambda^{-2}r^2}{\Lambda^{-4}k} \quad (4.54)$$

and the potential is

$$\Phi(r,z) = \left[C_2 J_0(\Lambda^{-1}r) + \frac{-\Lambda^{-2} - 4A + A\Lambda^{-2}r^2}{\Lambda^{-4}k}\right] exp(-\Lambda^{-1}|z|) \quad (4.55)$$

So the potential at the center of the electron cloud $(r = 0, z = 0)$ is given by:

$$\Phi(0,0) = -e^2 \left[C_2 - \frac{\alpha}{8\pi a_H} - \frac{\alpha^3}{16\pi a_H}\right] \quad (4.56)$$

with $\lim_{r\to 0} J_0(\Lambda^{-1}r) = 1$

For obtaining the value of C_2, we have to find the behavior of our potential at the infinity, so one needed to solve the last differential equation without the second member, in order to get the asymptotic solution which is

$$\Phi_{\text{asymp}}(r,0) = -e^2 C_2 J_0(\Lambda^{-1}r) \quad (4.57)$$

After that, we have to calculate the limit of $\frac{\Phi_{\text{asymp}}(r,0)}{\Phi_{\text{Coulomb}}}$

$$\lim_{r\to\infty} \frac{\Phi_{\text{asymp}}(r,0)}{\Phi_{\text{Coulomb}}} = \lim_{r\to\infty} \left(\frac{C_2 J_0(\Lambda^{-1}r)}{r^{-1}}\right) \quad (4.58)$$

with $J_0(\Lambda^{-1}r) = \frac{\sin(\Lambda^{-1}r)}{\Lambda^{-1}r}$

So

$$\lim_{r\to\infty} \frac{\Phi_{\text{asymp}}(r,0)}{\Phi_{\text{Coulomb}}} = \lim_{r\to\infty} \left(\frac{C_2}{B}\sin\left(\Lambda^{-1}r\right)\right) = [-1,1] \tag{4.59}$$

We choose

$$C_2 = -\frac{1}{2\Lambda} \tag{4.60}$$

Our potential will be:

$$\Phi(0,0) = -e^2\left[-\frac{\Lambda^{-1}}{2} - \frac{\alpha}{8\pi a_H}\right]$$

$$= \frac{e^2}{a_H}\left[\frac{1}{\alpha} + \frac{\alpha}{8\pi}\right] \tag{4.61}$$

4.5. The acceleration factor:

Any shift $U_e \ll E$ of the interaction potential energy $V(r)$

$$V(r) = \frac{Z_1 Z_2 e^2}{r} - U_e \tag{4.62}$$

accelerates the fusion cross section of hydrogen isotopes by a factor $f(E)$. The shielding effect reduces the Coulomb barrier and increases the penetration of the Coulomb barrier. Thus, it increases the cross section of nuclear fusion reactions. With $\sigma(E) = S(E)E^{-1}exp(-2\pi\eta)$, where $2\pi\eta = 2\pi Z_1 Z_2 e^2/\hbar v = 31.29 Z_1 Z_2\sqrt{\frac{\mu}{E}}$ is the Sommerfield parameter, ($Z_1$and Z_2 = charge numbers of the interacting nuclei in the entrance channel, μ= reduced mass in amu, E=center of mass energy in kev), and assuming a constant astrophysical $S(E)$factor over a relatively small energy interval, the enhancement ration f in fusion cross section is:

$$f(E) = \frac{\sigma(E+U_e)}{\sigma(E)} \tag{4.63}$$

$$f(E) = \frac{E}{E+U_e}\frac{exp[-2\pi\eta(E+U_e)]}{exp[-2\pi\eta(E)]} \tag{4.64}$$

For $U_e \ll E$ it reduces to

$$f(E) = exp\left[\pi\eta\frac{U_e}{E}\right] \tag{4.65}$$

In the strong magnetic field, the electron screening cloud is deformed in the sense that it becomes compressed perpendicular and parallel to the magnetic field. In the present work, this approximation has been tested for various fields and energies and the results are compared with those of ref [Lio00].

Therefore if the target hydrogen nuclei are in such magnetic field, the reaction is going to be accelerated by a factor

$$f(E) = exp\left[\pi\eta\frac{U_e(0,0,\alpha)}{E}\right] \tag{4.66}$$

Figure 4.2 depicts the acceleration of the pp reaction for various magnetic fields and interaction energies; figure 4.3 represents the acceleration factor obtained in ref [Lio00].

4.6. Heyl versus BES calculation

Let us now compare the BES and Heyl potential energies. The Taylor series for Heyl potential is as follows:

$$\Phi^{\mathrm{Heyl}}(0,0) = \frac{e^2}{a_H}\frac{2}{\sqrt{2\pi}}\left[\frac{4}{3} - \frac{1}{3}\alpha + \frac{2}{15}(\alpha-1)^2 - \frac{2}{35}(\alpha-1)^3 + \cdots\right] \tag{4.67}$$

The zero order BES potential can be written:

$$\Phi^{\mathrm{BES}}(0,0) = \frac{3e^2}{8\pi a_H}\left[\frac{8}{3\alpha} + \frac{\alpha}{3}\right] \tag{4.68}$$

If we limit ourselves for the first two terms, we note that the first term in our potential is proportional to the inverse of alpha no similar term exists in Heyl potential. For the second term we see that it is positive in our work, while is it negative in Heyl potential. This justifies the jump in the value of f for large magnetic field values (e.g $B = 10^{12}G$) as shown in Figure 4.4.

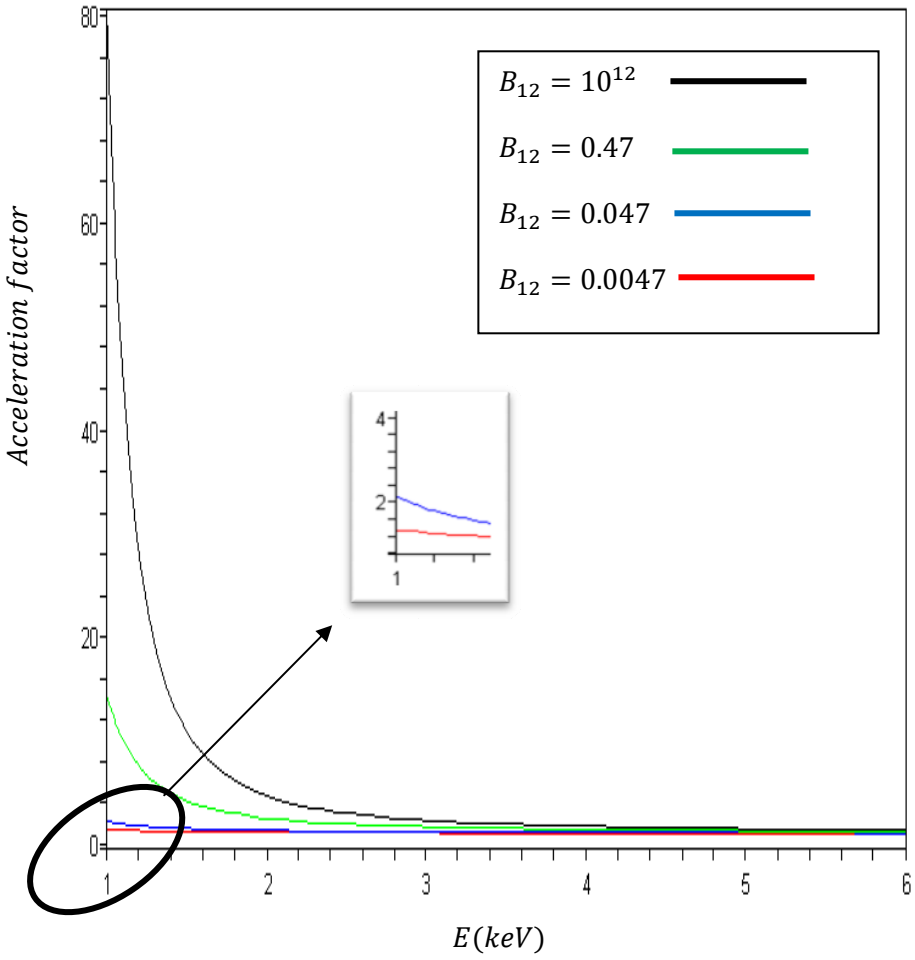

Fig4.2: *The acceleration (screening) factor f in BES model with respect to the relative interaction energy of two fusing protons for various super strong magnetic fields(in units of $10^{12}G$).*

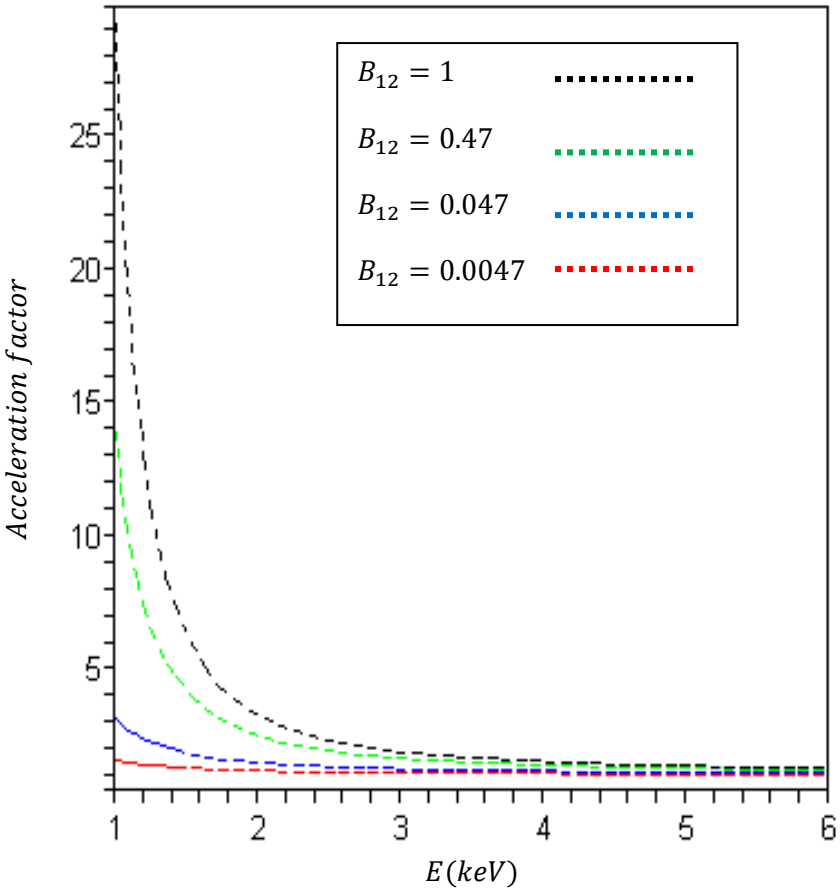

Fig4.3: *The acceleration (screening) factor taken from [Lio00].*

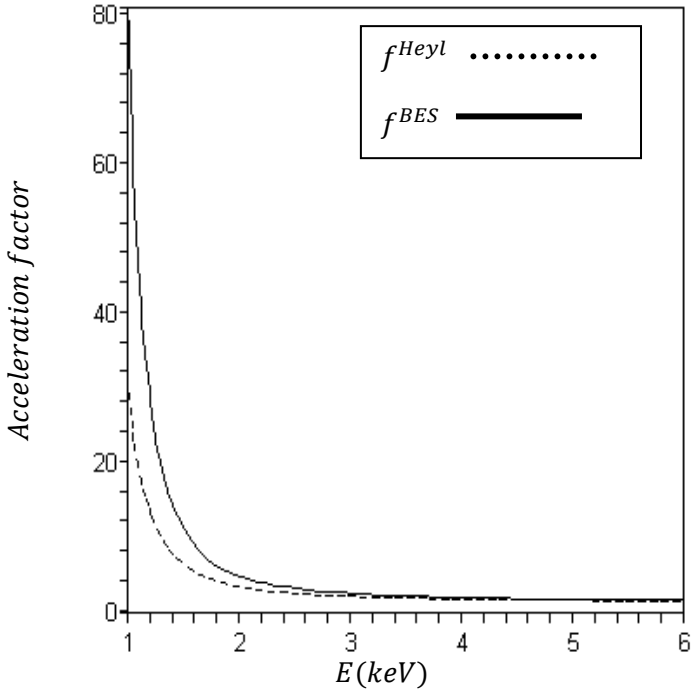

Fig4.4: *Comparison between the two models calculation with* $B = 10^{12}G$.

Chapter 5

SCREENED ALPHA DECAY IN SUPERSTRONG MAGNETIC FIELDS AND DENSE ASTROPHYSICAL PLASMAS

5.1. Introduction : Basic alpha decay processes

Alpha radioactivity has been known for a long time in heavy nuclei, the alpha particles were first identified as the least penetrating of the radiations emitted by naturally radioactive materials.

The spontaneous emission of an α particle can be represented by the following process:

$$ {}^{A}_{Z}X_{N} \rightarrow {}^{A-2}_{Z-2}X'_{N-2} + \alpha \tag{5.1} $$

The alpha particle, as was shown by Rutherford is a nucleus of ${}^{4}_{2}He$ consisting of two neutrons, and two protons. To understand the decay process, we must study the conservation of energy, linear momentum and angular momentum.

Let's consider the conservation of energy in the alpha decay process, we assume the initial decaying nucleus X to be at rest. Then the energy of the initial system is just the rest energy of X, $m_X c^2$. The final state consists of X' and alpha; each of which will be motion, thus the final total energy is $m_{X'}c^2 + T_{X'} + m_\alpha c^2 + T_\alpha$, where T represents the kinetic energy of the final particles. Thus conservation of energy gives:

$$ m_X c^2 = m_{X'}c^2 + T_{X'} + m_\alpha c^2 + T_\alpha \tag{5.2} $$

Or

$$ (m_X - m_{X'} - m_\alpha)c^2 = T_{X'} + T_\alpha \tag{5.3} $$

The quantity on the left side of equation (5.3) is the net energy released in the decay, called the Q value

$$ Q = (m_X - m_{X'} - m_\alpha)c^2 \tag{5.4} $$

Q values can be calculated from atomic mass tables because even though equation (5.4) represents a nuclear process. The electron masses will cancel in the subtraction. When the masses are in atomic mass units (u), expressing c^2 as 931.502 Mev/u. gives Q values directly in Mev. [Kra88]

The Q value is also equal to the total kinetic energy given to the decaying fragments:

$$Q = T_{X'} + T_{\alpha} \tag{5.5}$$

If the original nucleus X is at rest, then its linear momentum is zero; and conservation of linear momentum then requires that X' and alpha move with equal and opposite moment in order that the final total momentum also be zero:

$$\overrightarrow{p_X} + \overrightarrow{p_{X'}} = \vec{0} \tag{5.6}$$

Alpha decays typically release about 5Mev of energy. Thus for both X'and alpha, $T \ll mc^2$ and we may safely use nonrelativistic kinematics. Writing $T = \frac{P^2}{2m}$ and using equation (5.5) and (5.6) gives the kinetic energy of the alpha particle in terms of Q value:

$$T_{\alpha} = \frac{Q}{\left(1 + \frac{m_{\alpha}}{m_{X'}}\right)} \tag{5.7}$$

Which:

$$T_{\alpha} = \frac{A-4}{A} Q \tag{5.8}$$

Typically, the alpha particle carries about 98% of the Q value, with the much heavier nuclear fragments X' carrying only about 2%.

The kinetic energy of an alpha particle can be measured directly with a magnetic spectrometer and so the Q value of a decay can be determined.

5.2. Theory of alpha emission:

The general features of figure (5-1) can be accounted for by a quantum mechanical theory developed in 1928 almost simultaneously by Gamow and Gurney and Condon. In this theory an alpha particle is assumed to move in a spherical region determined by the *daughter* nucleus. The central feature of this one body model is that the alpha particle is preformed inside the parent nucleus. Actually there is not much reason to believe that alpha particle exists separately within heavy nuclei, nevertheless, the theory work quite well, especially for even-even nuclei. This success of the theory does not prove that alpha particles are preformed but merely that they behave as if they were.

Figure (5-1) shows a plot, suitable for proposes of the theory of the potential energy between the alpha particle and the residual nucleus for various distances between their centers. The horizontal line Q is the disintegration energy. Note that the Coulomb potential is extended inward to a radius R and then arbitrarily cut off. The alpha radius can be taken as the sum of the radius of the residual nucleus and of the alpha particle. There are three regions of interest. In the spherical region $r < R$ we are inside the nucleus and speak of a potential well of depth $-V_0$; where V_0 is taken as a positive number. Classically the alpha particle can move in this region, with a kinetic energy $Q + V_0$ but it cannot escape from it. The annular shell region $R < r < r_c$ form a potential barrier because here the potential energy

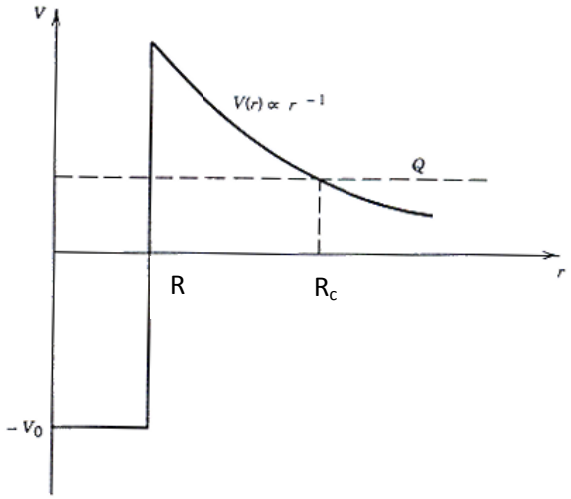

Fig5.1. *Relative energy of alpha particle, daughter-nucleus system as a function of their separation.*

is higher than the total available energy Q. Classically the alpha particle cannot enter this region from either direction, just a tennis ball dropped from a certain height cannot rebound higher. In each case the kinetic energy would have to be negative. The region $r > r_c$ is a classically permitted region out side the barrier.

From the classical point of view, an alpha particle in the spherical potential well would sharply reverses its motion energy time it tried to pass beyond $r = a$. Quantum mechanically, however, there is a chance of leakage or *tunneling* through such a barrier. This barrier accounts for the fact that alpha unstable nuclei do not decay immediately. The alpha particle within the nucleus must present itself again and at the barrier surface until it finally penetrates.

The barriers also operates in reverse, in the case of alpha particle scattering by nuclei. Alpha particles incident on the barrier from outside the nucleus usually scatter in the Coulomb field if the incident energy is well below the barrier height. Tunneling through the barrier, so that the nuclear force between the particle and target can cause nuclear reactions, is a relatively improbable process at low energy. The theoretical analysis of nuclear reactions induced by charged particles uses a formalism similar to that of alpha decay to calculate the barrier penetration probability. Fusion reactions, such as those responsible for the energy released in stars, also are analyzed using the barrier penetration approach [Kra88].

The disintegration constant of an alpha emitter is given in the one body theory by:

$$\lambda = fP \tag{5.9}$$

where f is the frequency with which the alpha particle presents itself at the barrier and P is the probability of transmission through the Coulomb barrier.

Equation (5.9) suggests that the treatment is going to be semiclassical in that the discussion of the situation for $r < R$ is very *billiard ballish* [Kra88]. A rigorous wave-mechanical treatment however, gives about the same results for this problem. The quantity f is roughly of the order of $\frac{v}{R}$ where v is the relative velocity of the alpha particle as it rattles about inside the nucleus. We can find v from the kinetic energy of the alpha particle for $r < R$.

The barrier penetration probability P must be obtained from a quantum mechanical calculation. The Coulomb barrier of figure (5.2) has height B at $r = R$ where

$$B = \frac{1}{4\pi\varepsilon_0}\frac{zZe^2}{R} \tag{5.10}$$

In this expression the alpha particle has charge ze and the daughter nucleus, which provides the Coulomb repulsion, has charge $Z'e = (Z - z)$e. the height of the barrier thus varies from $(B - Q)$ above the particle's energy at $r = R$ to zero at $r = r_c$, and we can take a representative average height to be $0.5(B - Q)$. For a typical heavy $(Z = 90; R = 7.5fm)$, the barrier height B is about 34 Mev, the radius b is

$$r_c = \frac{1}{4\pi\varepsilon_0}\frac{zZ'e^2}{Q} \tag{5.11}$$

And for a typical case of a heavy nucleus with $Q = 6\ Mev$, $r_c = 42\ fm$ thus:

$$P = \exp(-2K1/2(r_c - R)) \tag{5.12}$$

where $K = \sqrt{2m(V_0 - E)/\hbar^2}$

The exact quantum mechanical calculation is very similar in spirit to the crude estimate above. The probability to penetrate each infinitesimal barrier, which extends from $r\ to\ r + dr$ is:

$$dP = \exp(-2\sqrt{2m(V_0 - Q)/\hbar^2}\,)dr \tag{5.13}$$

The probability to penetrate the complete barrier is:

$$P = \exp(-G) \tag{5.14}$$

where the *Gamow factor* G is:

$$G = \sqrt{\frac{2m}{\hbar^2}}\int_R^{r_c}\sqrt{(V(r) - Q)}\,dr \tag{5.15}$$

which can be evaluated as:

$$G = \sqrt{\frac{2m}{\hbar^2 Q}}\frac{zZ'e^2}{4\pi\varepsilon_0}[arc\ cos\sqrt{x} - \sqrt{x(1-x)}] \tag{5.16}$$

where $x = \frac{R}{r_c} = Q/B$. The quantity in brackets in equation (5.16) is approximately $\frac{\pi}{2} - 2\sqrt{x}$ when $x \ll 1$, as is the case for most decays of interest. Thus the result of the quantum mechanical calculation for the half-life of alpha decay is:

$$t_{1/2} = 0.693\frac{R}{c}\sqrt{\frac{mc^2}{2(V_0+Q)}}exp\left\{2\sqrt{\frac{2m}{\hbar^2 Q}}\frac{zZ'e^2}{4\pi\varepsilon_0}\left(\frac{\pi}{2} - 2\sqrt{\frac{Q}{B}}\right)\right\} \tag{5.17}$$

If one makes a comparison between (5.17) and Geiger-Nutall law, we find the same results between the two formulas.

5.3. Screened alpha decay in a terrestrial environment

Let us assume that the parent nucleus is fully ionized (unscreened). During alpha decay, outside the range of the nuclear forces, the α particle ($^4_2He_2$) experiences only the repulsive Coulomb potential of the daughter nucleus ($^{A-4}_{Z-2}X'_{N-2}$) so the interaction energy is:

$$V_c(r) = \frac{2(Z-2)e^2}{r} \tag{5.18}$$

The maximum height of the barrier will of course be:

$$V_0 = \frac{2(Z-2)e^2}{R} \tag{5.19}$$

where R is the minimum distance between the daughter nucleus and α particle roughly given by

$$R = 1.3\left[(A-4)^{1/3} + 4^{1/3}\right] fm \tag{5.20}$$

The α decay half-life $T_{1/2}^{NSC}$ of an unscreened heavy nucleus is inversely proportional to the penetration factor $P(E_\alpha)$ given by the WKB method:

$$P(E_\alpha) = exp\left[-\frac{2\sqrt{2\mu}}{\hbar}\int_R^{r_c(E_\alpha)}\sqrt{V_c(r)-E_\alpha}dr\right] \tag{5.21}$$

where the kinetic energy of the α particle is:

$$E_\alpha = \left[\frac{A-4}{A}\right]Q_n \tag{5.22}$$

and the classical turning point is corresponds by:

$$V(r_c) = E_\alpha \tag{5.23}$$

One assumes that throughout the decaying process, the atomic cloud of the parent nucleus remains undisturbed so that the daughter nucleus is screened by the same cloud as the parent one and the α particle is emitted fully ionized; the neutral daughter atom will be assumed to have $Z-2$ electrons.

According to previous studies [Ass87], we can always define a screening enhancement factor (SEF) so that

$$f_\alpha(Z,A,Q_n) = \frac{P^{SC}(E_\alpha+U_e)}{P^{NSC}(E_\alpha)} \geq 1 \tag{5.24}$$

where $P^{SC}(E_\alpha+U_e)$is the screened penetration factor and $P^{NSC}(E_\alpha)$ is the unscreened one. Note that the kinetic energy E_α in equation (5.24) refers to the unscreened nucleus.

Since $T_{1/2}{\sim}P^{-1}(E_\alpha)$, we can write the following for the screened $T_{1/2}^{SC}(Z,A,Q_n)$ and the unscreened $T_{1/2}^{NSC}(Z,A,Q_n)$ half-lives:

$$T_{1/2}^{SC}(Z,A,Q_n) = \frac{T_{1/2}^{NSC}(Z,A,Q_n)}{f_\alpha(Z,A,Q_n)} \tag{5.25}$$

In this work, we will show that the screening effect reduces the half-life of the decaying nucleus. This is of course as expected, since the screening cloud reduces the Coulomb barrier thus easing the way of the α particle out of the parent nucleus. In Fig 5.2, a simplified picture of the screened alpha decay is drawn. According to that figure, the Coulomb potential practically vanishes at distances further than three screening radii.

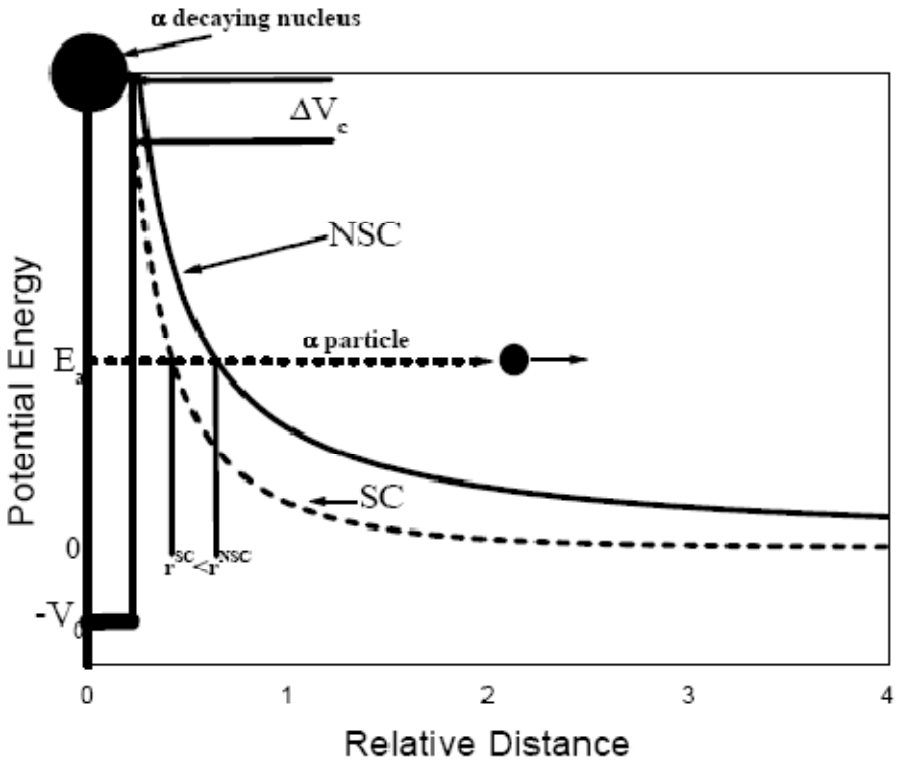

Fig5.2: *A simplified picture of screened alpha decay taken form [Lio03]. The alpha particle is emitted with a (relative) kinetic energy E_α, while the screened (r^{sc}) and unscreened (r^{NSC}) classical turning points are also shown.*

5.4. Magnetically catalyzed alpha decay in magnetars:

Nowadays, there is a growing body of evidence [Pav02] for a population of neutron stars with magnetic fields of the order of $10^{15}G$, which is much larger than the typical magnetic field of a neutron star (i.e.,10^{15}G). These "magnetars" are distinguished from radio pulsars and accreting binary neutron stars not only by the strength of their field but also by the fact that their decaying magnetic field is their primary energy source. Moreover, recent observation [Pav02] provide strong evidence for the validity of the old hypothesis that two separate classes of astronomical x-ray sources- the soft gamma repeaters and the anomalous x-ray pulsars are actually different manifestations of this peculiar type of star. The giant magnetic field of magnetars has a significant and observable effect on quantum electrodynamic processes operating near the star. It can also support strong and persistent electrical currents, which alter the spin down of the star and contribute to the continuous glow of X rays and optical light observed in between outbursts.

In large magnetic field, such as those existing in the atmospheres of neutron stars, atomic clouds are compressed both perpendicular and parallel to the magnetic field direction [The00]. The effects of giant magnetic fields ($B \geq 10^{12} G$) on hydrogen and helium atoms have been extensively studied by many authors ([Lio00],[Lio03],[Ban74],[Rud83],[Kel72]). Various studies have appeared focusing on such topics as the nuclear fusion [Hey96]. In the present work, we will consider the effects of such magnetic field on alpha decay processes.

The present study will exclusively focus on the perturbation of half-lives due to atomic (tunneling) effects allowing for an extra perturbation term due to nuclear effects. We have particularly chosen Uranium as it is thoroughly used as cosmochronological tools.

5.4.1. The BMSC Potential (Batna Magnetic Screened Coulomb Potential):

Let us consider the heavy hydrogenoid atom of an alpha decaying element (like ${}^{235}_{92}U$) which is under the influence of such an ultrastrong magnetic field. We will disrecard all exchange, thermal, and relativistic effects as a first approximation and adopt the usual supermagnetic field notation (see §4.3.1). Moreover the parent and the daughter nuclei are considered spinless, just like alpha particle.

The Batna magnetic screened Coulomb potential will given by:

$$V_{sc}(r,B) = V_c(r) - \Phi(r,z,B) \tag{5.26}$$

where $V_c(r)$ is given by equation (5.18) and $\Phi(r,z,B)$ has been obtained in Chapter 4. So

$$V_{sc}(r,B) = \frac{2(Z-2)e^2}{r} + 2e^2\left[C_2 J_0\left(\Lambda^{-1}r\right) - \frac{\Lambda^2}{k}\right] exp\left(-\Lambda^{-1}|z|\right) \tag{5.27}$$

with $C_2 = -\frac{\Lambda^{-1}}{2}$, $J_0(\Lambda^{-1}r) = \frac{\sin(\Lambda^{-1}r)}{\Lambda^{-1}r}$, $k = 2\pi a_H^2 a_z$, $a_z = \alpha a_H$, $\Lambda^{-1} = \frac{2}{a_z}$

5.4.2. The magnetically enhanced screening factor

In order to calculate the effect of the magnetic field on α half lives, we consider the potential (5.27) in the simple case $z = 0$.

$$V_{sc}(r,B) = \frac{2(Z-2)e^2}{r} + 2e^2\left[-\frac{\sin(\Lambda^{-1}r)}{2r} - \frac{\Lambda^2}{k}\right] \tag{5.28}$$

Figures (5.3), (5.4), (5.5) and (5.6) show the reduction of the Coulomb barrier as function of the magnetic field.

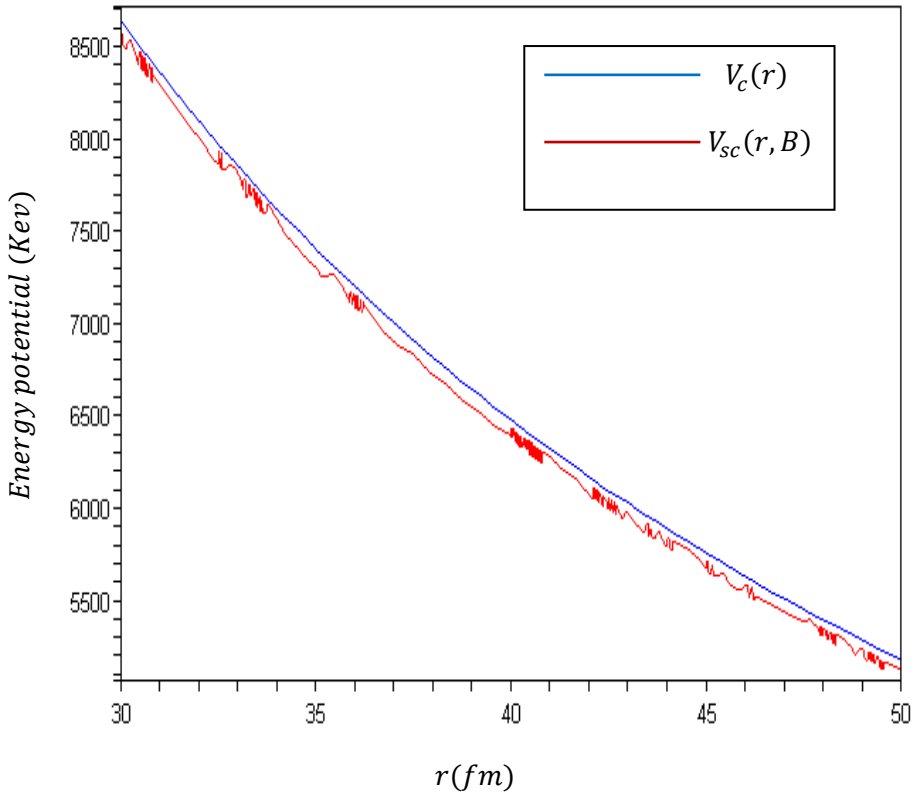

Fig5.3:*Comparison between the two potential with* $B = 4.7 \times 10^9 G$.

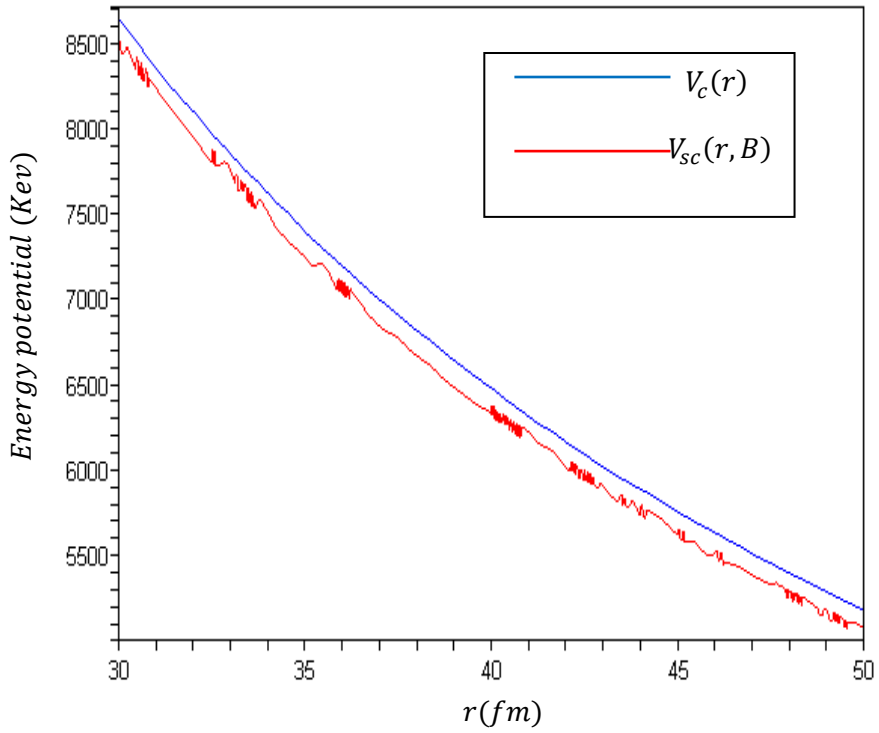

Fig5.4: *Comparison between the two potential with* $B = 4.7 \times 10^{10} G$.

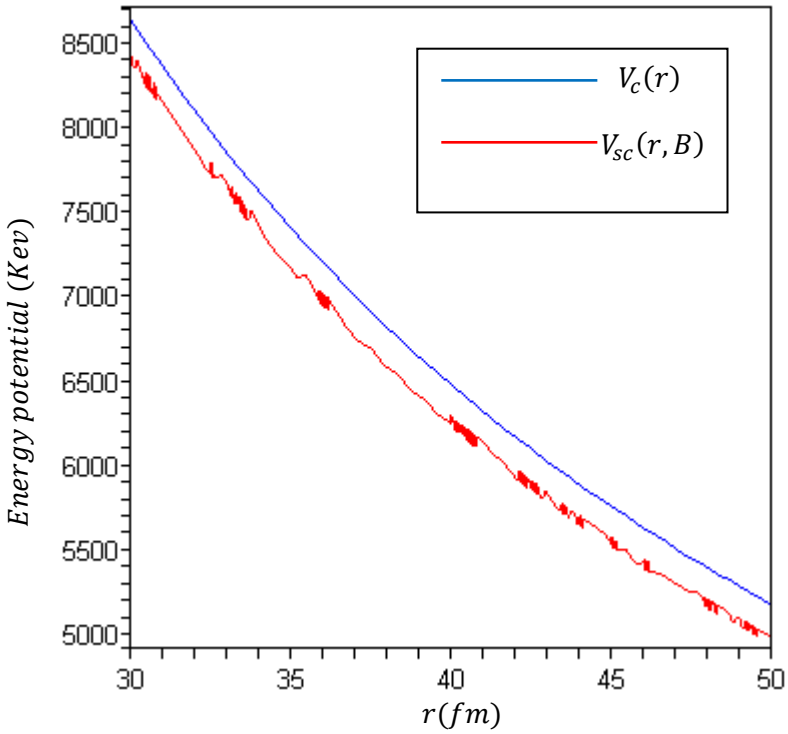

Fig5.5: *Comparison between the two potential with* $B = 4.7 \times 10^{11} G$

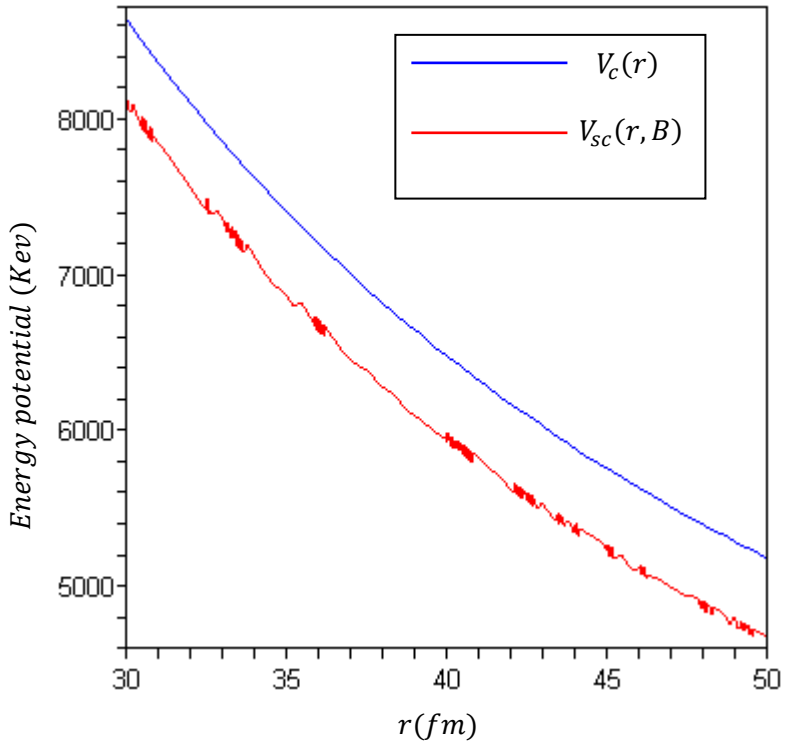

Fig5.6:*Comparison between the two potential with* $B = 10^{12}G$.

The magnetically enhanced screening effect will be given by the screened versus the unscreened penetration factor:

$$f(Z,A,B) = exp\left[-\frac{2\sqrt{2\mu}}{\hbar}\left(\int_R^{r_c(E_\alpha,B)}\sqrt{\frac{2(Z-2)e^2}{r}+2e^2\left[-\frac{\sin(\Lambda^{-1}r)}{2r}-\frac{\Lambda^2}{k}\right]-E_\alpha}\,dr - \int_R^{r_c(E_\alpha)}\sqrt{\frac{2(Z-2)e^2}{r}-E_\alpha}dr\right)\right] \quad (5.29)$$

We have first calculated the classical turning point r_c given by $V_{sc}(r,B) = E_\alpha$ for different values of B. One notices (as expected) that r_c decreases with B (Table 5.1). The mathematical program "Maple" has been used to calculate r_c and f.

B(G)	R (fm)	$r_c(E_\alpha)$ (fm)	$r_c(E_\alpha, B)$(fm)
4.7×10^9	10.04015152	43.9400519	43.9379064
4.7×10^{10}	10.04015152	43.9400519	43.15784749
4.7×10^{11}	10.04015152	43.9400519	42.73201305
10^{12}	10.04015152	43.9400519	42.03294800

Table5.1 *: Results of the numerical calculation of* $r_c(E_\alpha,B)$ *and* $r_c(E_\alpha)$.

The integration results show a clear reduction of α half lives for strong magnetic field (Table 5.2).

B(G)	$\mathbf{f(Z, A, B)}$
$\mathbf{4.7 \times 10^{9}}$	1.12
$\mathbf{4.7 \times 10^{10}}$	3.37
$\mathbf{4.7 \times 10^{11}}$	10.33
$\mathbf{10^{12}}$	102.14

Table5.2 : *Results of the numerical integrations.*

5.5. Screened alpha decay in dense astrophysical plasmas

5.5.1. The linear plasma shielding:

Thermonuclear reaction rates in stars are increased over their laboratory analogs because of the presence of the dense electron gas. The net negative charge surrounding each nucleus reduces the coulomb repulsion to a value smaller than $\frac{Z_1 Z_2 e^2}{r}$. This reduction makes the penetration of the coulomb barrier easier, which in turn increases the cross section in comparison with the cross section between bare nuclei having the same relative velocity at infinity.

Each nucleus, even though completely ionized, attracts neighboring electrons somewhat. There will exist, on the average, some sphere around each nucleus Z which contains enough negative charge to neutralize the cloud. This sphere should not be thought of as containing just Z free electrons, for it will usually contain other positive nuclei with sufficient electrons to neutralize them as well (the Debye-Hückel ion sphere). Only if the average coulomb energy between neighboring particles is greater than kT (usually not the case) will the cloud tend to reduce to Z free electrons. When two nuclei Z_1 and Z_2 approach each other, the shielding charge density introduces a perturbing potential on the coulomb one. We write the total coulomb interaction energy as

$$U_{tot}(r_{12}) = \frac{Z_1 Z_2 e^2}{r_{12}} + U(r_{12}) \tag{5.30}$$

where $U(r_{12})$ obviously represents the added interaction due to shielding.

The shielding cloud must be at least as large as the average interparticle distance and perhaps much larger, and $U(r_{12})$ will change by large amounts only over distances of the order of the radius of the shielding cloud. Equation (5.31), on the other hand, shows explicitly that the penetration factor depends upon the integral of $(U_{tot} - E)$ between the classical turning point R_0 and the nuclear radius *R*.

$$P = \left[\frac{V(R)-E}{E}\right] \exp\left\{-\frac{2\sqrt{2\mu}}{\hbar}\int_R^{R_0}[V(r) - E]\, dr\right\} \tag{5.31}$$

Since reactions are most favored for the energy E_0, a characteristic classical turning radius is of the order

$$R_0 = \frac{Z_1 Z_2 e^2}{E_0} \tag{5.32}$$

This turning radius is usually much less than the radii of the shielding clouds. Thus the shielding interaction $U(r_{12})$ must be essentially constant over the relevant range of interparticle distances for which both articles are near the center of the shielding clouds. To good approximation $U(r_{12})$ in the penetration factor can be replaced by U_0, the shielding potential at the origin. The potential is shown schematically in Fig 5.7.

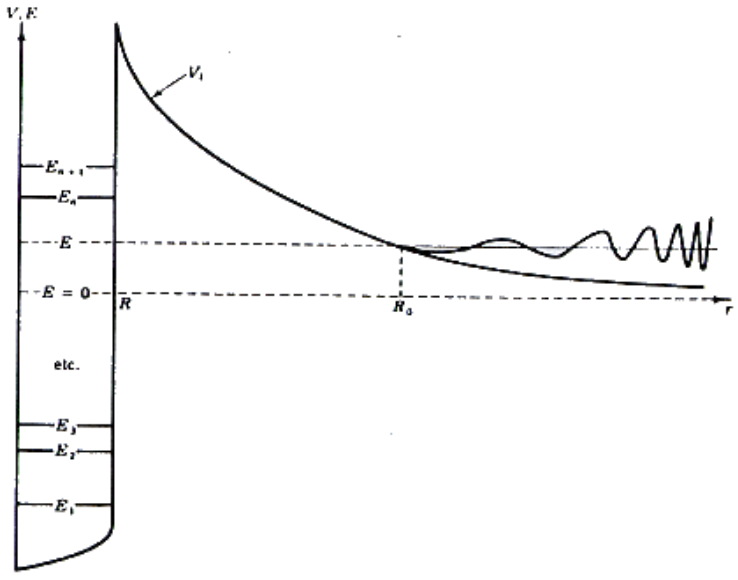

Fig 5.7: *the effective radial potential*

5.5.2. Linear plasma shielding model

Thermonuclear reactions constitute the source of stellar energy and all the laws that govern such reactions deserve to be thoroughly investigated. The enhancing influence of stellar plasmas on thermonuclear reaction rates has been studied by many authors ([Lio03] and reference therein) who derive the Screening Enhancement Factor (SEF) by which the reaction rates are multiplied in order to take into account screening effects. The most widely used screening model is the Salpeter's weak screening model (linear plasma shielding).

Consider a test charge q in a dense plasma, in the thermal equilibrium, the probability of particle being in a state with energy E is ~ to $exp\left(\frac{-E}{KT}\right)$, where K is Boltzmann's constant.

Since probability and number density are proportional to each other in a gas, and since the energy of a particle is simply $E = q\Phi$, we may write for electron and ion densities

$$n_e = Aexp\left(\frac{\mathrm{e}\Phi}{KT}\right) \tag{5.33}$$

Note that the ions do not move but form a uniform background of positive charge, so; we have:

$$n_i = n_0 \tag{5.34}$$

where n_0 is the density of ions before the point charge arrived.

At infinity $\Phi \to 0$ and there is no applied field to disturb the equilibrium between ions and electrons, so, we have $A = n_0$. To determine the potential $\Phi(r)$ we just use Poisson's equation

$$\nabla^2\,\Phi = -\rho = -n_0 e\left(exp\left(-\frac{\mathrm{e}\Phi}{KT_i}\right) - 1\right) + q\delta(\vec{r}) \tag{5.35}$$

We will suppose that: $\frac{\mathrm{e}\Phi}{\mathrm{KT_i}} \ll 1$, and $\frac{\mathrm{e}\Phi}{KT_e} \ll 1$, keeping only the first two term to obtain a new approximate version of Poisson's equation:

$$\nabla^2\,\Phi = n_0 e^2\,\frac{\Phi}{KT} + q\delta(\vec{r}) \tag{5.36}$$

The solution of the last equation is

$$\Phi(r) = \frac{-q}{r}\exp\left(\frac{-r}{R_D}\right) \tag{5.37}$$

Where, R_D *is the Debey length* $R_D = \sqrt{\frac{KT}{2n_0e^2}}$ and $q = (Z-2)$.

If we write equation (5.37) as Taylor series, we get then:

$$\Phi(r) = -\frac{q}{r} + \frac{q}{R_D} - \frac{q}{2}\frac{r}{{R_D}^2} + \frac{1}{6}\frac{qr^2}{{R_D}^2} \tag{5.38}$$

5.5.3. The nonlinear plasma shielding

The double aim of this section is: a) to prove that the definition of the weak screening limit used by Salpeter, which actually yields the Debye-Hückel potential, forbids the use of the potential inside the tunneling region, b) the region of validity of the Debye-Hückel potential in stellar plasmas is obtained by given a new model for weakly screened thermonuclear reactions, which is capable of taking in account the non linear screening effect.

We expend equation (5.35) by using the Taylor series of the exponential function, taking account the nonlinear term,

$$\frac{2}{r}\frac{d\Phi}{dr} + \frac{d^2\Phi}{dr^2} = 2n_0e\left[\frac{\mathrm{e}\Phi}{KT} + \frac{1}{4}\left(\frac{\mathrm{e}\Phi}{KT}\right)^2\right] \tag{5.39}$$

This differential equation has not analytical solution. In order to get an approximate solution, the quadratic term in Φ will be replaced by

$$\psi(r) = \frac{1}{r}(\alpha_0 + \alpha_1 r + \alpha_2 r^2 + \cdots) \tag{5.40}$$

If we assume that the nonlinear terms is small, one needs simply to keep the first terms in its expansion. So, equation (5.39) will be written as:

$$\frac{2}{r}\frac{d\Phi}{dr} + \frac{d^2\Phi}{dr^2} = 2n_0e\left[\frac{\mathrm{e}\Phi}{KT} + \frac{1}{4}\frac{e^2}{K^2T^2}\left(\frac{1}{r}\alpha_0 + \alpha_1\right)^2\right] - q\delta(r) \tag{5.41}$$

Using Mathematical Maple Calculation, we will get

$$\Phi(r) = -\frac{c_1}{r} exp\left(\sqrt{a} \times r\right) - \frac{\alpha_0^2 \sqrt{a} \cosh\left(\sqrt{a} r\right) ab}{a^{3/2}} - \frac{B\alpha_0^2 \ln(a) \sinh\left(\sqrt{a} r\right) a + \sqrt{a} B \alpha_1 (2\alpha_0 + \alpha_1 r)}{a^{3/2} r} \quad (5.42)$$

We write the exponential as Taylor's series, then we get

$$\Phi(r) = \frac{\left(q + 2\alpha_1 \alpha_0 b R_D^2\right)}{r} + \frac{q}{2R_D^2} r - \frac{eb}{R_D^2} r^2 - b(\alpha_0{}^2 \ln(a) + \alpha_1^2 R_D^2) \quad (5.43)$$

where we have defined the constants

$$\begin{cases} a = \frac{2e^2 n_0}{KT} = \frac{1}{R_D^2} \\ b = \frac{1}{2} \frac{e^3 n_0}{(KT)^2} \\ c_1 = -q = -(Z-2) \end{cases} \quad (5.44)$$

in the equation (5.42).

We will choose

$$\begin{cases} \alpha_0 = \frac{2KT}{e} \\ \alpha_1 = \frac{1}{R_D} \sqrt{\frac{2KT}{e}} \end{cases} \quad (5.45)$$

The equation (5.43) will be

$$\Phi(r) = \frac{(Z-2) + 2\sqrt{2n_0 e} R_D}{r} + C_0 r + C_1 r^2 + C_3 \quad (5.46)$$

where

$$C_0 = \frac{Z-2}{2R_D^2} \quad (5.47)$$

$$C_1 = 2R_D{}^2 e n_0 \quad (5.48)$$

$$C_3 = \frac{1}{R_D} \ln(R_D) - 1 \quad (5.49)$$

If we make a comparison between (5.46) and (5.38), we see the difference between the two potential which is the appearance of the term $\frac{2\sqrt{2n_0 e}R_D}{r}$. this difference is explaining by the fact taking account the quadratic term in equation (5.39).

5.5.4. Effect of non-linear plasma screening

Let us consider a heavy alpha decaying nucleus ${}^{A}_{Z}M_N$ in fully ionized multicomponent plasma which is at thermodynamic equilibrium, in order to derive screening corrections in our alpha decay study. The enhanced screening effect will be given by the screened versus the unscreened penetration factor:

$$f(Z,A,n_0) = exp\left[-\frac{2\sqrt{2\mu}}{\hbar}\left(\int_R^{r_c(E_\alpha,B)}\sqrt{\frac{((Z-2)+2\sqrt{2n_0 e}R_D)e^2}{r}+\left(\frac{Z-2}{2R_D^2}\right)e^2 r \atop +2R_D e^3 n_0 r^2+\left(\frac{1}{R_D}\ln(R_D)-1\right)e^2-E_\alpha}\,dr - \int_R^{r_c(E_\alpha)}\sqrt{\frac{(Z-2)e^2}{r}-E_\alpha}dr\right)\right] \tag{5.50}$$

The last expression, shows the effect of a non linear plasma shielding which is the reduction of alpha decay half lives.

Conclusion

The electron screening acceleration of laboratory fusion reactions at astrophysical energies is an unsolved problem of great importance to astrophysics.

We have studied the screening enhancing effect at low energy fusion reactions using two approaches. In the first one the expression of the electron charge density is given, a prior while in the second one it is calculated from the wave functions. We have shown that the presence of excited states increase the astrophysical factor the reaction $^{3}He(^{3}He, 2p)\,^{4}He$.

By means of the proposed model, the effect of a superstrong magnetic field on Hydrogen fusion reactions is investigated here and applied on the $(D-D)$ fusion reaction. This study gives a high screening energy for hydrogen fusion reactions

Electron screening effects in alpha decay processes is studied, applying a formalism which has been used in the study of astrophysical fusion reactions. We have derived alternative analytic SEF formulae for stellar medium. The effects of superstrong magnetic fields (such as those of magnetars) on alpha decay is a reduction of the relevant half-life. This effect, may possible have notable implications on heavy elements abundances and the cosmochronological models that rely.

Finally, it has been shown, that alpha decay half-lives in dense astrophysical plasmas can be reduced. A simple formula has been developed to take into account the non linear term of Poisson equation.

REFERENCES

[And94] W.J. Anderson,H.J.Haubold, & A.M.Mathai, arXiv:astro-ph/9402020v1. 08 Feb 1994.

[Arn00] M. Arnould & M. Samyn, la physique nucléaire en astrophysique, Ecole Joliot-Curie de physique nucléaire 2000.

[Ass87] H.J. Assenbaum, K. Langanke and Rolfs, Z. Phys. A237 (1987) 461.

[Aud72] J. Audouze & S. Vauclair, L'astrophysique nucléaire, Presses universitaires de France, 1972.

[Ban74] B.Banerjee,D.H. Constantinescu & P.Rehak, Phys. Rev. D,10, (1974), 2384.

[Ben89] G. Bencze, Nuc. Phys A 492 (1989) 459-472.

[Bin87] J. Binney & S. tremaine, Galactic Dynamics, Princton University Press, 1987.

[Bra83] B.H Bransden & C.J.Joachain, Physics of atoms and molecules, British library 1983.

[Cha92] G. Chanmugam; Annu.Rev. Astron. Astrophys.1992, 143-145.

[Cla86] D.D. Clayton, Principles of stellar evolution and nucleosynthesis, McGraw-Hill,NewYork,1986.

[Eng88] S. Engstler, a Krauss, K. Neldner and M. Scharff, C.Rolfs and Schrôder, Phys.lett. B202 (1988) 179.

[Hey96] J. S.Heyl & L. Hernquist, Phys.Rev.C,54, (1996), 5

[Kel72] D.C.Kelly & V.Canuto. Ast.&. Space science 17. (1972), 277-291

[Kra87a] A. Krauss, H, W. Becker, H,P. Trauvetter and C. Rolfs, Nucl,Phys. A 465 (1987) 179.

[Kra87b] A. Krauss, H, W. Becker, H,P. Trauvetter and C. Rolfs, Nucl,Phys. A 467 (1987) 273-290.

[Kra88] K.S.Krane, Introductory nuclear physics, John wiley &sons,1988.

[Lai06] D. Lai,& A. K.Harding, arXiv: astro-ph/0606674v2,11Jul 2006.

[Lan67] L. Landau & E. Lifchitz, Quantum Mecanics, MIR Edition, 1967.

[Lio03] T.E. Liolios, Phys.Rev. C, 68, (2003), 015804.

[Lio01] T.E. Liolios, arXiv: nucl-th/0009071 v2 6 Jan 2001.

[Lio00] T.E. Liolios, Eur,phys J.A9,(2000),287-292.

[Pav02] G.G.Pavlov,V.E. Zavlin & D. Sanwal, arXiv:astro/ph0206024v2.11 Jun2002.

[Rau03] A.R.P.Rau, Astronomy inspired atomic and molecular physics, KLUWER ACADEMIC PUBLISHERS, New York 2003.

[Rol87] C.Rolfs, H.P. Trautvetter and W.S.Rodney, Rep. Prog.Phys.50 (1987) 233.

[Rud83] H. Ruder, W.Rösner, H. Herold & G. Wunner. Phys.Rev. A,28, (1983), 4.

[Str01] F. Streider. C Rolfs, Naturewissenschaften (2001) 461-467.